ANALYSIS AND IMPLEMENTATION OF OPTICAL FIBER SENSORS FOR PROCESS MONITORING OF COMPOSITE MATERIALS

A Thesis Submitted to
the Graduate School of Engineering and Sciences of
İzmir Institute of Technology
in Partial Fulfillment of the Requirements for the Degree of

MASTER OF SCIENCE

in Electronics and Communication Engineering

by
Anıl YILMAZ

December, 2016
İZMİR

We approve the thesis of **Anıl YILMAZ**

Examining Committee Members:

Assist. Prof. Dr. Kıvılcım YÜKSEL ALDOĞAN
Department of Electrical and Electronics Engineering, Izmir Institute of Technology

Prof. Dr. M. Salih DİNLEYİCİ
Department of Electrical and Electronics Engineering, Izmir Institute of Technology

Prof. Dr. Metin TANOĞLU
Department of Mechanical Engineering, Izmir Institute of Technology

Assist. Prof. Dr. Osman AKIN
Department Of Mechatronics Engineering, İzmir Katip Çelebi University

Assist. Prof. Dr. Fatih YAMAN
Department of Electrical and Electronics Engineering, Izmir Institute of Technology

27/12/2016

Assist. Prof. Dr. Kıvılcım YÜKSEL ALDOĞAN
Supervisor, Department of Electrical and Electronics Engineering
Izmir Institute of Technology

Prof. Dr. M. Salih DİNLEYİCİ
Head of the Department of
Electrical and Electronics Engineering

Prof. Dr. Bilge KARAÇALI
Dean of the Graduate School of
Engineering and Sciences

ACKNOWLEDGEMENTS

First of all, I would like to express my sincere gratitude to my supervisor Assist. Prof. Dr. Kıvılcım YÜKSEL ALDOĞAN for her support, motivation and scientific guidance throughout my master study and preparation of this thesis.

I would like to thank Ümit ALDOĞAN for his help and support during our laboratory studies.

I would like to acknowledge Dr. Damien Kinet and whole UMONS-SET team for providing us FBG sensors.

I am grateful to Prof. Dr. M. Salih DİNLEYİCİ, Assist. Prof. Dr. Osman AKIN and Assist. Prof. Dr. Fatih YAMAN for serving on my thesis committee.

I would like to express my gratitude to Prof. Dr. Metin TANOĞLU for allocating composite materials laboratory and involving to my thesis committee.

I'd like to thank my friend and colleague Ali YILMAZ for all his help and encouragement.

I also thank Osman KARTAV for his helps and patience during the composite material productions.

Special thanks to all my friends and family for their help and endless support during my master studies.

ABSTRACT

ANALYSIS AND IMPLEMENTATION OF OPTICAL FIBER SENSORS FOR PROCESS MONITORING OF COMPOSITE MATERIALS

The use of composite materials in many industrial applications and structures under high stress (airplane wings, unmanned air vehicles, wind turbines, etc.) has been exponentially growing thanks to their lightweight, superior strength, durability, and corrosion resistance. However, the unique mechanical properties of composite materials cannot be fully exploited without monitoring them when material is placed under constraints. It is essential to monitor their behavior not only in the field but also during manufacturing process to ensure the high quality of manufactured materials. For this purpose, the use of optical fiber sensing, particularly the embedding of fiber Bragg grating (FBG) sensors into composite materials has been gaining growing popularity thanks to various advantages of FBGs. In this context, the main purpose of this thesis is to demonstrate the feasibility of using optical fiber sensors for process monitoring (cure and resin flow) of fiber reinforced thermoset composite materials.

The first sensor type studied in the thesis was based on Fresnel reflection. The capability of monitoring the curing profile of liquid matrix (mixture of resin and hardener) has been demonstrated by the way of Fresnel reflection sensor interrogated by Optical Time Domain Reflectometry (OTDR). Then, FBG sensors were embedded into composite plates to measure the temperature change during resin injection and cure cycle, as well as determining the residual strain inside the material. In spite of the popularity of using FBG sensors, most recent researches clearly prove that there is still a lack of technical maturity in real life applications in interrogating embedded FBGs for strain measurements. There is still room for new sensing approaches. In the last part of the thesis, we proposed a novel method to interrogate fiber cavity ring-down (CRD) loop by using OTDR which makes this sensing approach more practical and cheaper than the conventional techniques. Thanks to these advantages, our proposed interrogation method can be implemented for strain measurements inside the composite materials as an alternative to the FBG sensors.

ÖZET

KOMPOZİT MALZEMELERDE PROSES GÖZETİMİ AMACIYLA FİBER OPTİK SENSÖRLERİN ANALİZ VE UYGULAMASI

Pek çok endüstriyel uygulamada ve yüksek mekanik gerilime maruz yapılarda (uçak kanatları, insansız hava araçları, rüzgar türbinleri, vb.) kompozit malzemelerin kullanımı sağladıkları hafiflik, üstün sağlamlık, dayanıklılık ve korozyon direnci gibi özellikler sayesinde gittikçe artmaktadır. Ancak kompozit malzemelerin bu avantajlı özellikleri tam anlamıyla faydalanabilmek için malzemenin yük altındaki davranışının izlenmesi gerekmektedir. İmal edilen malzemelerin yüksek kalitesini sağlamak için malzemenin davranışlarını yalnızca sahada değil, aynı zamanda üretim süresince de izlemek gereklidir. Bu amaçla, fiber optik algılamanın kullanılması, özellikle fiber Bragg grating (FBG) sensörlerinin kompozit malzemelere yerleştirilmesi, FBG'lerin çeşitli avantajları sayesinde popülarite kazanmaktadır. Bu bağlamda, bu tezin temel amacı, fiber takviyeli termoset kompozit malzemelerin üretiminin izlenmesi (kürlenme ve reçine akış) için optik fiber sensörlerin uygulanabilirliğini göstermektir.

Tezde incelenen ilk sensör tipi Fresnel yansımasına dayanmaktadır. Sıvı matrisin (reçine ve sertleştirici karışımı) kürlenme profilinin izlenebilmesi, Optik Zaman Alanı Reflektometresi (OTDR) tarafından sorgulanan Fresnel yansıma sensörü yolu ile gösterilmiştir. Ardından, FBG sensörleri, reçine enjeksiyonu ve kürlenme döngüsü sırasında sıcaklık değişimini ölçmek ve malzemenin içindeki artık gerinimi (residual strain) belirlemek için kompozit plakalara gömülmüştür. FBG sensörlerinin popülerliğine rağmen, yapılan araştırmalar, gerinim ölçümleri sırasında FBG sorgulama yöntemlerinin pratikte teknik olarak yeterli olgunlukta olmadığını göstermektedir. Yeni sensör sorgulama yaklaşımları için çalışmalar hala devam etmektedir. Tezin son bölümünde, fiber kavite ring-down (CRD) döngüsünü, OTDR kullanarak, konvansiyonel tekniklerden daha pratik ve ucuz bir yöntemle sorgulanmasını sağlayan yeni bir yöntem önerilmiştir. Bu yöntemin, sağladığı avantajlar sayesinde, kompozit malzemelerin içindeki gerinimleri ölçmek için (FBG sensörlerine alternatif olarak) uygulanabileceği gösterilmiştir.

TABLE OF CONTENTS

LIST OF FIGURES

Figure **Page**

LIST OF TABLES

Table **Page**

LIST OF ABBREVIATIONS

CRD	Cavity Ring-Down
EDFA	Erbium-Doped Fiber Amplifier
EMI	Electromagnetic Interference
FBG	Fiber Bragg Grating
FOS	Fiber Optical Sensor
OSA	Optical Spectrum Analyzer
OTDR	Optical Time Domain Reflectometer
RTM	Resin Transfer Molding
TLS	Tunable Laser Source

CHAPTER 1

INTRODUCTION

With increasing demands on technology, engineers always tried to improve their designs by using smarter materials and advanced technologies. In their designs, they have to consider productivity, optimal efficiency and cost-effectiveness. Improving technological designs brought up a new class of materials called composite materials.

Composite materials have been gaining a prominent position in marketplace over the last years thanks to their lightweight, superior strength, durability, and corrosion resistance compared to conventional materials [1]. The use of composite materials is highly favorable for the fabrication of heavily loaded structures thanks to their superior characteristics. The enormous potential of these materials has been the driving source behind the recent advances in many applications including aerospace, renewable energy production, automotive, etc. However, some critical issues related to the continuous monitoring of their gradual degradation under load are still being investigated around the world. Many groups have been working to develop novel technologies based on fiber optics for monitoring strain and damage state of the composite structure. Such a system detecting and interpreting adverse changes in the structure in service will play a crucial role in the full exploitation of the composite materials. Measuring strain distribution and loads on the composite materials is of great importance for many aspects. Not only for in-service applications, but also for the improvement of the production steps (e.g. cure monitoring of composite laminates) can benefit from the integrated structural monitoring.

There is a number of processing methods explored for the fiber reinforced composite materials. One of the manufacturing processes of structural composite components is vacuum-assisted resin infusion. In this manufacturing technique, fiber preforms (glass or carbon) are situated on mold and covered with a vacuum bag. Then resin is injected into the mold to saturate the fiber preforms. After the resin cures completely, the vacuum bag is opened and the final material is removed from the mold [1]. There are two critical processing steps in this method: the resin injection and curing (polymerization) stages. Thus, this manufacturing process must be fully controlled to

ensure that final product has high quality composite parts within acceptable tolerances [2].

Achieving these objectives requires advanced technologies to monitor the health of the material during and after production. This monitoring is highly needed to prevent potential damages and all kind of possible failures in advance. As a result of these demands, fiber optical sensors (FOS) become highly attractive technology for process monitoring of composite materials.

Huge number of advantages (low attenuation, small dimensions, immunity to electromagnetic interference (EMI) and electrically passive nature) made fiber optical sensors more popular and applicable than conventional counterparts. In addition, fiber optic sensors can be embedded and/or attached into composite materials without degrading the performance and life of the host structure. In this context, fast, reliable and cost-effective interrogation unit that can be implemented in many application areas is of paramount importance for optical fiber-based sensing systems.

Within the framework of this thesis, fiber optical sensor implementations into composite materials were studied. Additionally, a novel interrogation set-up was proposed to monitor a recently developed sensor technology; fiber cavity ring-down (CRD) loop. Fiber CRD loop technology has great advantages due to its simplicity and flexibility to implement different optical fiber sensors within the loop. This flexibility makes them practical for different parameter measurements such as temperature, pressure, and strain. In the framework of this thesis, a novel interrogation set-up for fiber CRD loop is proposed and the sensor's linear response is explored which is of particular interest in monitoring mechanical behavior of composite materials.

1.1. Thesis outline

This thesis is organized in four chapters. Their contents are summarized below to express the works done under this thesis study.

Chapter 2: In this chapter, an overview of fiber optical sensors together with their classification is provided. It also explains composite material production methods. Afterwards, the engineering aspects and development stages of sensor implementation (Fresnel reflection and FBG) into composite material production monitoring are explained.

Based on preliminary measurements, it is shown that the cure monitoring of resin can be implemented (based on Fresnel reflection sensor) by measuring refractive index of the material. Also, temperature changes and residual strain can be monitored during composite material production stages by the way of embedded FBG sensors.

Chapter 3: This chapter is devoted to a novel interrogation approach of fiber cavity ring-down loop technology. Our proposed method presented in this chapter is capable of measuring attenuation values imposed by a sensor head independently from the environmental temperature fluctuations. Operation principles are explained in detail. Experimental proof-of-concept is presented. Experimental work shows that our proposed CRD loop interrogation approach based on OTDR has strong conveniences (robust, low-cost, easy to use) compared to previous configurations.

Finally, chapter 4 sums up the all completed works and it discusses future perspectives of these sensor applications.

CHAPTER 2

IMPLEMENTATION OF OPTICAL FIBER SENSORS FOR MONITORING OF COMPSITE MATERIALS

2.1. Fiber optical sensors

Although already largely spread since 90s, the fiber optic technological revolution has not only been valuable for telecommunication applications. Indeed, the huge potential of optical fibers has also been exploited, during the last two decades, for sensing purposes. Fiber optic sensors have found an important role in applications where conventional electronic sensors could not be implemented, hence, they are fast replacing their conventional electronics counterparts in many industrial sectors like civil engineering, space/aviation, health and logistic. The optical fiber based sensors benefit from the advantages inherent to the use of the optical fiber. Typically, these advantages are: its low attenuation, high bandwidth, immunity to electromagnetic interference (the fiber is a dielectric), lightness and small transverse dimensions. All these features allow the emergence of applications where conventional sensors are not appropriate like, for instance, in hazardous environments where the explosion risk is a major concern, or in applications where non-intrusive properties are required [3].

Fiber-optical sensors can also be classified according to three categories: the sensing location, the operating principle and the application, as seen in table 2.1.

Table 2.1. Fiber optical sensors categories [4]

Category	Class	Properties
sensing location	point sensors	with a single sensor tip
	distributed sensors	the measurement all along the fiber
	quasi-distributed senso	in between point and distributed
operating principle	intensity sensors	
	polarzation sensors	
application fields	physical sensors	for temperature, stress, velocity, etc.
	chemical sensors	for pH, gas analysis, etc.

Different sensing locations give us opportunity to realize diverse sensor prototypes. In addition to table 2.1, figure 2.1 represents the sensor location classes.

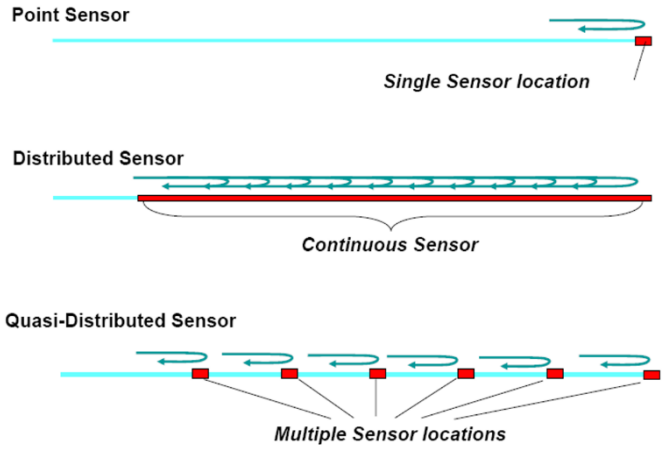

Figure 2.1. Sensor classes with respect to sensing locations [3]

In this part of the work, we implemented both point (Fresnel Reflection-based) and quasi-distributed (Fiber Bragg Gratings) sensors for the monitoring of composite materials

2.1.1. Fiber Bragg grating sensors

Discovery of photo-sensitivity in optical fibers brought out a novel class of optical fiber sensors: Fiber Bragg Gratings (FBG). Photosensitivity was observed for the first time in 1978 in germanium doped silica fiber at the Communications Research Centre (CRC) in Ottawa, Canada. Scientist K.O. Hill and his co-workers observed that the amplitude of the reflected light significantly increased after a long exposure to an intense visible light. Spectral measurements have showed that a permanent and periodic refractive index modulation had been obtained in the fiber core [5].

After this discovery, there have been intensive research and development efforts for FBGs in the past decade. What makes them quite useful in sensor applications is their sensitivity to distinct physical and chemical properties such as; temperature, stress, strain, vibration, chemical gasses, etc.

2.1.1.1. Principle of fiber Bragg gratings

A fiber Bragg grating can be produced by generating periodic and permanent modification in the refractive index of the fiber core [6]. Photosensitive property of optical fibers make it possible to generate periodic and permanent modification by several UV interference patterns. There are some parameters that have important roles in fiber Bragg grating theory. The grating length L is the length of refractive index modulation along the fiber core. The refractive index modulation and periodicity are implemented by δn and Λ [5] [6].

An FBG pattern can be thought as a selective mirror in wavelength domain [5]. In other words, FBG can transmit a specific range of wavelengths while a small portion of light is reflected back through the gratings. This reflected wavelength is called Bragg wavelength and defined by the equation (2.1) [7].

$$\lambda_{Bragg} = 2n_{eff}\Lambda \qquad (2.1)$$

n_{eff} is the effective refractive index of optical fiber. Physically, for each period of the FBG, a weak reflection is produced due to a variation of the refractive index value. An important reflection can be obtained when all the weak contributions are added in phase [5] [6] [7]. Operating principle of FBG can be understood more clearly with the configuration in figure 2.2.

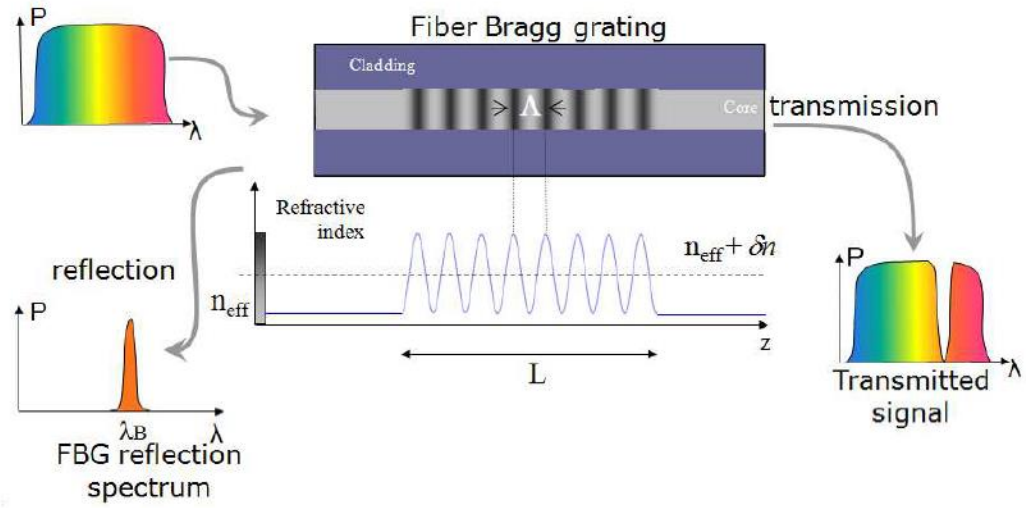

Figure 2.2. Operating principle of fiber Bragg gratings [3]

Reflection spectrum (R) of an FBG with length L can be formulated as [5]

$$R = \frac{K^2 \sinh(\alpha L)^2}{K^2 \cosh(\alpha L)^2 - \sigma^2} \qquad (2.2)$$

These parameters can be defined by the following relationships [5]

$$K = \frac{\pi v \delta n}{\lambda} \qquad (2.3)$$

$$\sigma = 2\pi n_{eff}\left(\frac{1}{\lambda} - \frac{1}{\lambda_{Bragg}}\right) + \frac{2\pi\delta n}{\lambda} \qquad (2.4)$$

$$\alpha = \sqrt{K^2 - \sigma^2} \qquad (2.5)$$

The effective refractive index of the fiber is denoted by n_{eff}. K is defined as coupling coefficient and changing with wavelength λ (fringe visibility v is equal to 1). The self-coupling coefficient σ is related to the Bragg wavelength of the FBG as in equation (2.4). By using equations (2.2) to (2.5) a sample FBG reflection spectrum is simulated (cf. Figure 2.3).

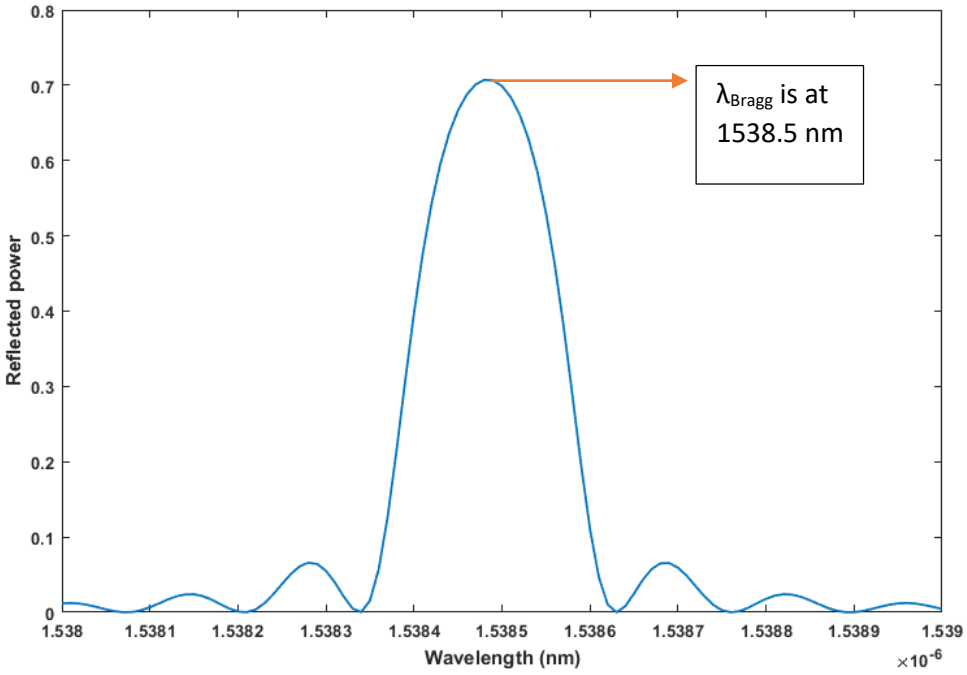

Figure 2.3. Simulated FBG reflection spectrum (L=6 mm, n_{eff}=1.4513)

Figure 2.4 represents one of the FBGs measured reflection spectrum in our laboratory. This spectrum was obtained from the optical spectrum analyzer (OSA) through the Keysight VEE Pro software (communication between OSA and computer was held by the way of GPIB IEEE-488 connection).

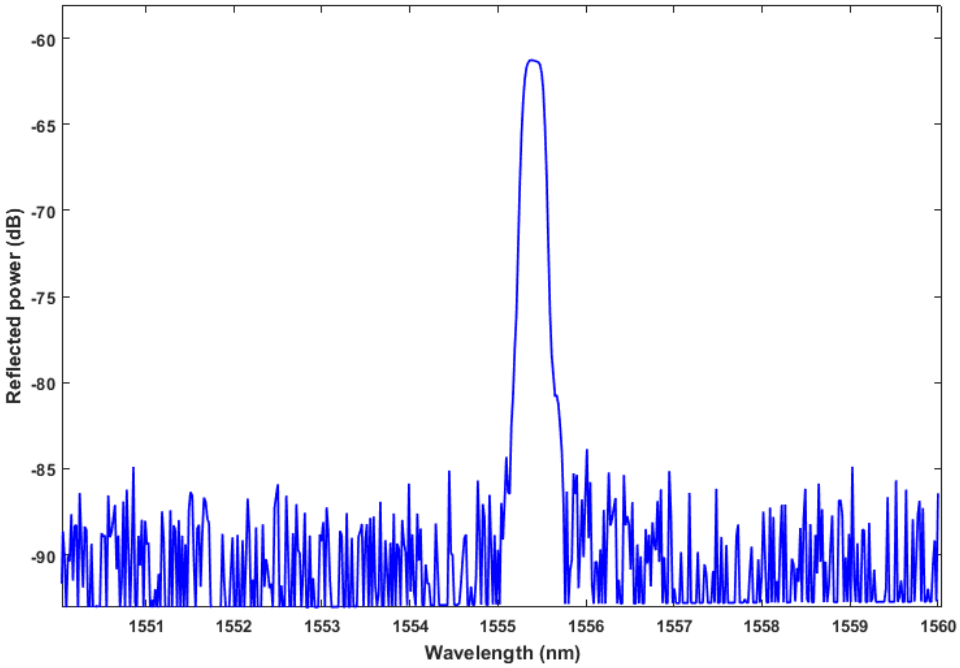

Figure 2.4. Sample FBG reflection spectrum from OSA (λ_{Bragg}=1555.5 nm)

2.1.1.2. Temperature and strain sensitivities of fiber Bragg gratings

Equation (2.1) implements that; the Bragg wavelength depends on the effective refractive index of the core and the spatial periodicity of the gratings. The effective refractive index or grating period can be changed due to the thermo-optic and strain-optic effect [5].

$$\frac{\Delta\lambda_{Bragg}}{\Delta T} = \lambda_{Bragg}\left(\frac{1}{n_{eff}}\frac{dn_{eff}}{dT} + \frac{1}{\Lambda}\frac{d\Lambda}{dT}\right) \qquad (2.6)$$

Equation (2.6) represents the shift amount of the Bragg wavelength due to the temperature effect. This shift in the wavelength comes from the modification of grating spacing and refractive index. ΔT and $\Delta\lambda_{Bragg}$ are the temperature change and corresponding Bragg shift [5].

- $\frac{1}{n_{eff}}\frac{dn_{eff}}{dT}$ is defined as thermo-optic coefficient and its approximate value is 8.6 10^{-6} K^{-1} for the germanium doped silica core optical fiber [5].
- $\frac{1}{\Lambda}\frac{d\Lambda}{dT}$ is defined as the thermal coefficient of optical fiber and its approximate value is equal to 0.55 10^{-6} K^{-1} for silica[5].

It is obvious that refractive index change is more dominant effect. The temperature sensitivity of Bragg wavelength is around 10pm/ºC [3].

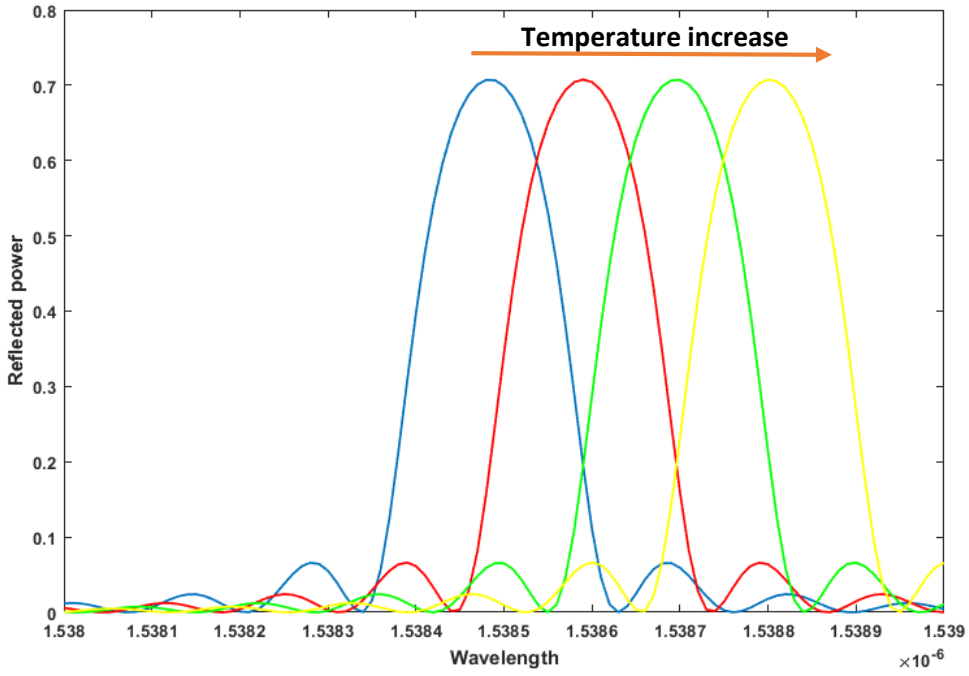

Figure 2.5. Bragg wavelength shift under the temperature change

Figure 2.5 is obtained from a MATLAB simulation to show the Bragg wavelength shift under temperature change. Rise in the temperature clearly results in increasing the Bragg wavelength.

$$\frac{\Delta\lambda_{Bragg}}{\Delta\varepsilon} = \lambda_{Bragg}\left(\frac{1}{n_{eff}}\frac{dn_{eff}}{d\varepsilon} + \frac{1}{\Lambda}\frac{d\Lambda}{d\varepsilon}\right) \qquad (2.7)$$

Equation (2.7) represents the effect of longitudinal strain on an optical fiber. The Bragg shift in uniform FBG with respect to $\Delta\varepsilon$ is equal to 1.12 pm/με [5].

2.1.1.3. Simultaneous temperature and strain influence

Any change in wavelength due to an external perturbation to the grating is the sum of temperature and strain effects. Thus, temperature and strain effects has to be separated in sensing applications when two perturbations have to be simultaneously measured and for which only one of them is of interest. A single grating written into a standard single-mode fiber exhibits a strong sensitivity to both temperature and strain perturbations.

There are several methods to eliminate this effect. In our experimental works reference fiber Bragg grating method is used as it is the easiest method to implement. This method basically uses a strain-free reference fiber Bragg grating to compensate the temperature effect. Implementation of this method in our experiments is explained in more detail in the section 2.4 [5].

2.1.2. Fresnel reflection based sensors

Fresnel reflection based sensors are good candidates to measure the refractive index of materials and can be classified as point sensors with single sensing point. This sensor application is inspired by basic optical phenomenon called Fresnel reflection. Figure 2.6 shows its basic operating principle.

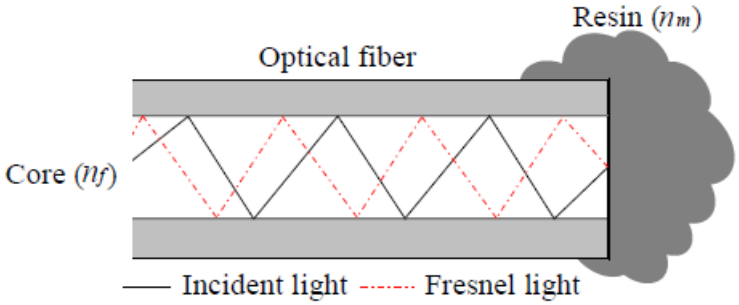

Figure 2.6. Fresnel reflection due to external medium (resin as represented in the figure) [8]

Fresnel reflection based sensor system determines the refractive index from the Fresnel reflection of the cleaved end of an optical fiber. With this cleaved face of the fiber, a small change in refractive index modifies the intensity of the reflected light. For a fiber tip (perpendicularly cleaved fiber end), the power reflection coefficient is given as [9];

$$R = \left|\frac{n_f - n_m}{n_f + n_m}\right|^2 \qquad (2.8)$$

In equation (2.8) n_f is the effective index of the fiber, and n_m is the refractive index of the material surrounding the fiber.

2.2. Composite Materials

2.2.1. Definition

In general, composite material consists of two main constituent: reinforcement fiber and matrix [10]. Composite material composed of these constituents and it has superior properties than those of its constituents. For example, if the final material needs to be fire-resistant, a fire-retardant matrix can be used in the development stage so that it has this property. While combining different types of compounds, the designer has endless amount of options to create a final material that meets his best requirements.

Composite materials are utilized across a broad range of areas, particularly the aerospace, marine and automotive sectors [11]. The combination of a high strength fiber network and supporting matrix material, either a thermoset, e.g. epoxy or thermoplastic, e.g. polypropylene, results in a material with a high strength to weight ratio [10]. They are typically used in safety critical and high technology applications.

2.2.2. Application fields

The construction of safe automobiles, aircrafts with high range, and extremely light machine components can be achieved with composite materials (cf. figure 2.7).

Figure 2.7. Application fields of composite materials [11]

Composite materials are mostly chosen for fabrication of various parts of different structures such as aircraft tails, wings, propellers, helicopter rotor blades, wind turbine

blades and parts of racing cars, boats, and sports equipment etc. Composite materials become a significant topic for researchers as the demand on smart materials is increasing. Some modern airplanes are built with composites rather than metal including the new Boeing 787 Dreamliner [12].

2.2.3. Advantages of composite materials

Variety of mechanical advantages make composite materials more popular to use than other conventional materials. Having high strength and low weight of composite materials comparing non-composite materials become prominent advantages. Additionally, composite material exhibits good damage tolerance. These characteristics are reasons for using composites in safety critical and high technology applications e.g aerospace, automotive, marine and civil engineering [13]. Some fundamental advantages can be listed as follows [12] [14]:

- Light weight*:* Composites are lighter in weight comparing to conventional metal or wooden materials. Weight is always an important parameter to think about while designing aircrafts and vehicles such as trucks in order to reduce the needed amount of fuel.
- High strength: It is possible to design the composites to be stronger than aluminum or steel. Metal materials can be equally strong in all directions whereas composites can be designed to be stronger in a specific direction.
- High-Impact strength: Composite materials are capable of absorbing impacts which makes them useful in bulletproof vests, panels and to shield military vehicles.
- Radar Transparent*:* Radar signals can easily pass right through the composites. This property is used while designing U.S Air Force's B-2 stealth bomber that is nearly invisible to radar [14].

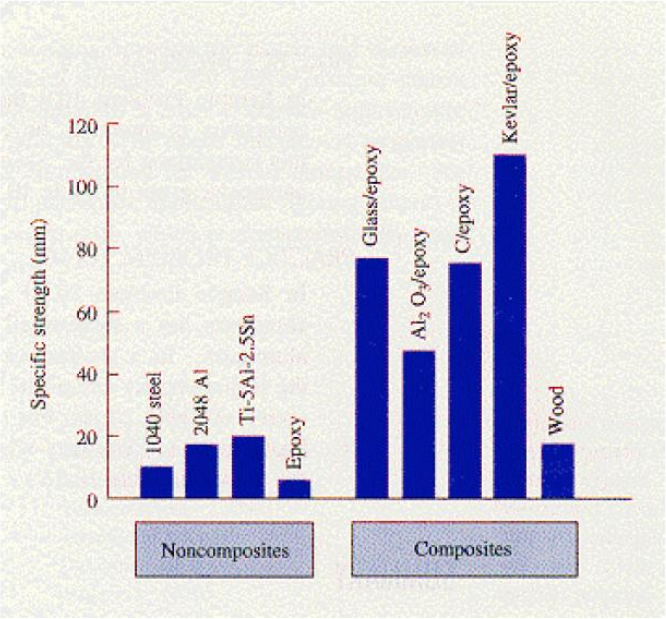

Figure 2.8. Comparison of the composite materials properties to traditional materials [14]

2.2.4. Composite components

Composite materials basically consists of two main components; reinforcement fiber and matrices [10].

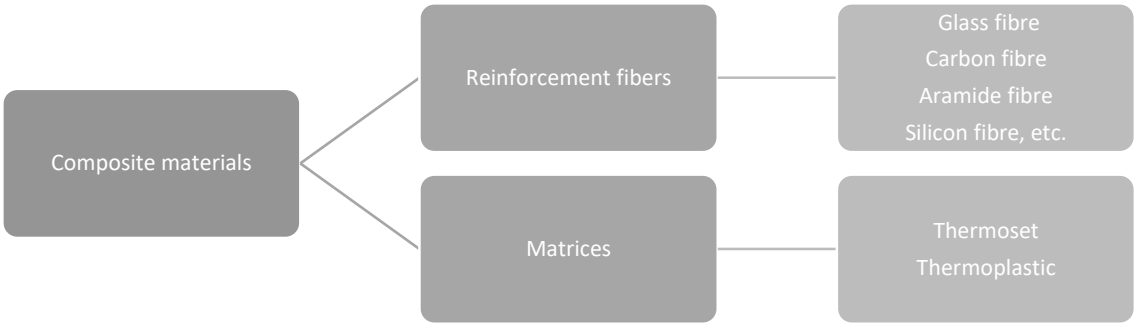

2.2.4.1. Reinforcement fibers

The reinforcement fibers in the composites are originally synthetic fibers developed for the textile industry [13]. The essential role of fibers in composites is to

improve the mechanical properties. These mechanical properties are explained in detail in the section 2.2.3.

The reinforcement elements (fibers), that are widely used, are listed as follows [10] [13]:

- Carbon fiber (high performance)
- Glass fiber (cost effective)
- Aramide fibers
- Silicon fibers (high temperature applications)
- Metalic fibers (copper or aluminum, for their electrical properties)
- Mineral fibres (silica for fire resistance property)

2.2.4.2. Matrices

The basic functions of matrix material are to hold the reinforcement fibers together in place and to ensure an even distribution of strain between the reinforcement fibers. In composite materials, there are two kinds of matrices used; thermoplastic and thermoset resins. Most composite materials are produced based on thermoset resins. Table 2.2 shows a basic comparison for the two resin types [13].

Table 2.2. Matrices comparison

Resin type	Process temperature	Process time	Use temperature	Solvent resistance	Toughness
Thermoset	Low	High	High	High	Low
	↑	↓	↑	↑	↓
Thermo plastic	High	Low	Low	Low	High

The most common used thermoset resin types are epoxy and polyester [10]. Having a high solvent resistance, low cost and requiring low process temperature make thermoset resins more preferable in composite material productions. Thermoset resins are in liquid form and their curing stage is a polymerization process which exhibits an exothermic reaction. Table 2.3 display some basic thermoset resin types including their temperature range and application fields.

Table 2.3. Common thermoset resin types [10]

Thermoset Resin	Typical Temperature Range $(F)^0$	Application Fields
Polyester	140-300	Commercial (pipe, tank marine, automotive) Energy (wind tribunes)
Vinyl Ester	140-300	Commercial (pipe, tank marine, automotive) Energy (wind tribunes)
Epoxy	180-400	Aerospace (aircraft, launch vehicles, marine, armor), Automotive, Medical, Oil and Gas industry (pressure vessels, drilling technologies)

Thermoplastic resins are generally used with short fiber reinforcements and they are found in solid form. By heating in an elevated temperature, they are melted and this softened matrix is ready to mix with reinforcement fiber to form the composite material. Polypropylene, nylon and polycarbonate are three common thermoplastic resin types [10].

2.2.5. Composite production techniques

There are several fabrication techniques. The most common methods are resin transfer molding and vacuum-assisted resin infusion method [1].

Resin transfer molding (RTM)

In the RTM technique, fiber reinforcements are packed into a mold that is possible to design in a desired shape. A second mold is used to clamp over the first mold and necessary space is created to inject the resin into the mold. Using a vacuum helps to flow

the resin all over the reinforcement material. Figure 2.9 can help to understand this process.

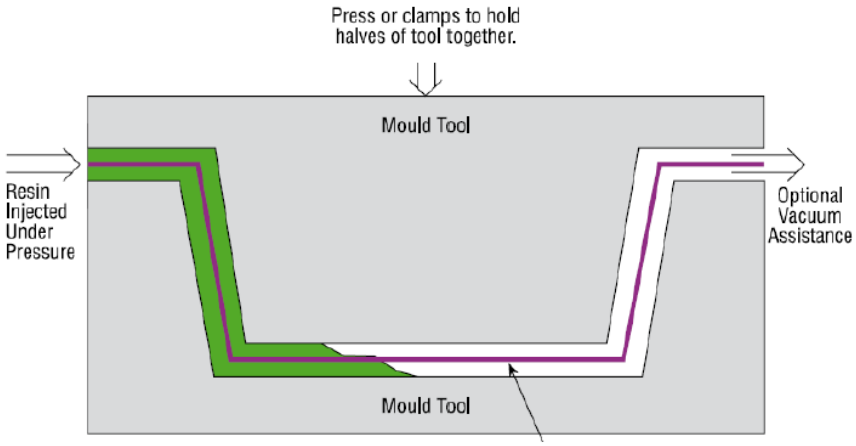

Figure 2.9. Resin transfer molding process [1]

This process requires high control of the resin flow due to the possibility of the un-impregnated areas. Currently, German automotive manufacturer BMW uses RTM technique in conjunction with robotic laydown fiber preforms to manufacture the body frame of the car [1].

Vacuum-assisted resin infusion

Unlike RTM, this method doesn't use a second mold, instead a vacuum bag is used. In this process, a permeable layer, such as peel ply is employed to distribute the resin throughout the parts quickly. The main advantage compared to RTM process is its simplicity and it requires low investment as only one mold surface is used. However, the lack of automation is the drawback of this method. Figure 2.10 represents this method clearly.

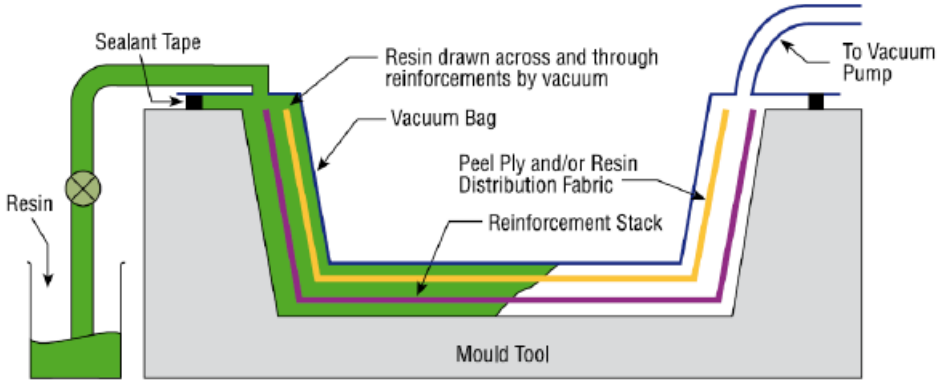

Figure 2.10. Vacuum-assisted resin infusion method [1]

Both of the aforementioned production methods are available in IZTECH Mechanical Engineering laboratories. Due to its simplicity and the cost efficiency, vacuum-assisted resin infusion method was used in our experimental works.

2.3. Experimental Work

2.3.1. Resin cure monitoring

Resin is the matrix component of composite materials to hold the reinforcement fibers together in place. Cure monitoring of resin is an important process to understand the curing stage of composite materials. It helps us to estimate the curing time for resin which is significant parameter to use the mold tools and time effectively in mass productions [2] [13]. There is an additional chemical compound required to cure the resin, called hardener. In order to understand the curing process of the resin, the Fresnel reflection based sensor application was implemented.

2.3.1.1. Experimental set-up for resin cure monitoring

For this experiment, a sample was prepared by mixing MSGLS L160 laminating epoxy with MGS H160 Hardener.

As interrogation unit, we used Optical Time-Domain Reflectometer (OTDR). It basically measures the back reflected signal. Figure 2.11 shows the experimental set-up for the resin cure monitoring.

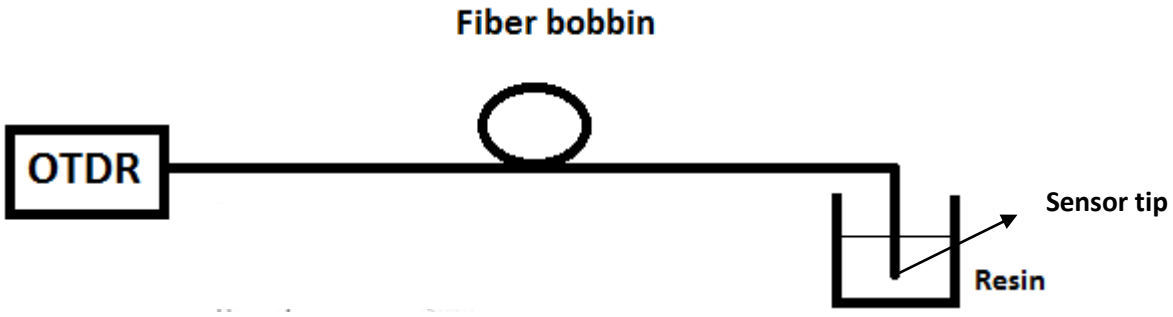

Figure 2.11. Experimental set-up for cure monitoring of resin

In this measurements, OTDR sends and receives optical pulses with 5 nm bandwidth at 1550 nm wavelength. Sample OTDR trace in the figure 2.11 demonstrates the events all along the fiber. When the sensor tip is exposed to the target material (resin in figure 2.11), the measured reflectivity (i.e. the end reflection peak corresponding to fiber-liquid interface appearing on the OTDR trace in figure 2.11, R_{end} in dB), can be used to calculate the refractive index value of the resin (n_m) [9]. In order to calculate refractive index n_m, we need to convert Eq. 2.8 into dB domain as;

$$R_{end} = 10\log\left|\frac{n_f - n_m}{n_f + n_m}\right|^2$$

$$\frac{R_{end}}{20} = \log\left|\frac{n_f - n_m}{n_f + n_m}\right|$$

$$10^{\frac{R_{end}}{20}} = \left|\frac{n_f - n_m}{n_f + n_m}\right|$$

$$n_m = n_f\left[\frac{1-10^{R_{end}/20}}{1+10^{R_{end}/20}}\right], n_f > n_m \quad , \quad n_m = n_f\left[\frac{1+10^{R_{end}/20}}{1-10^{R_{end}/20}}\right], n_f < n_m \qquad (2.9\text{-}10)$$

The distilled water was used for calibration purposes since its refractive index was known. Table 2.4 represents the reflection powers and refractive indexes of distilled water, hardener and epoxy. Refractive indexes were calculated by using the equation (2.9-2.10) in logarithmic domain.

Table 2.4. Calculated refractive indices regarding to measured reflections

Substance	**Reflection (dB) (Measured)**	**Refractive index (Calculated)**	**Refractive index (From data sheets)**
Distilled water	-26.4 (±0.2)	1.334	1.333
Hardener	-34.9	1.5219	1.5200-1.5230
Epoxy	-31.2	1.5513	1.5480-1.530

2.3.1.2. Resin cure monitoring results and discussions

OTDR was set to take automatic measurements in every 5 minutes until R_{end} values reached a steady state at the end of curing process. The change in reflection values and calculated refractive indeces of the resin and hardener mixture can be seen in the figure 2.12.

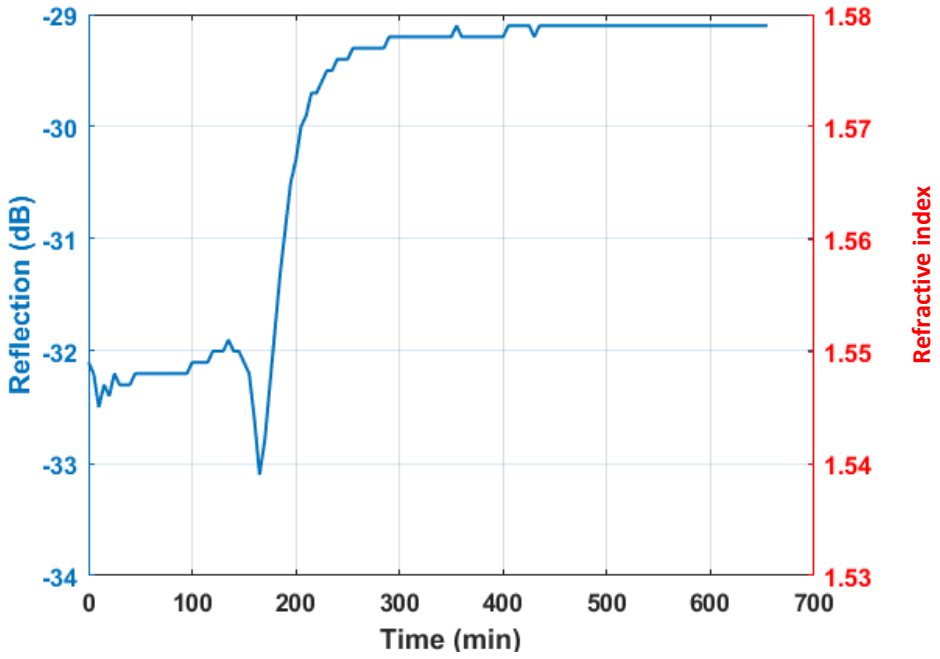

Figure 2.12. Fresnel reflection plot

The measured Fresnel reflections (R_{end}) were used in the equation 2.9 and 2.10 to calculate the refractive index values (n_m). We can precisely observe the starting time of curing process associated with the significant drop in Fig. 2.12. After an amount of time (approximately 2 hours), resin and hardener mixtures refractive index got stabilized. Additional observation during this measurement was the change in temperature. When the mixture started curing, a sudden temperature increase was observed. This is related with an exothermic reaction process occurred during curing. These experiments were preliminary steps in understanding the curing behavior of resin.

2.3.2. Monitoring of amplitude spectrum of FBG sensors during composite production

This part consists of the following sections; vacuum-assisted infusion technique performed in IZTECH, FBG sensor interrogation set-up and embedding the fiber Bragg grating sensors into a composite material for cure monitoring, discussion and results.

2.3.2.1. Vacuum-assisted infusion technique in IZTECH

We used vacuum-assisted infusion method in IZTECH Mechanical Engineering Departments Laboratory to produce composite materials. This method was realized with the help of laboratory assistants under the guidance of Professor Dr. Metin Tanoğlu.

Initial step is placing the reinforcement fibers layer by layer as in the figure 2.13. At this stage, the number of layers are selected for desired thickness. As we have interested in observing the curing cycle, we decided to make a simple square shape with 4 layers. Additionally, a protective zone has to be created around the fibers with a strong sticky tapes as shown in the figures 2.13 - 2.14.

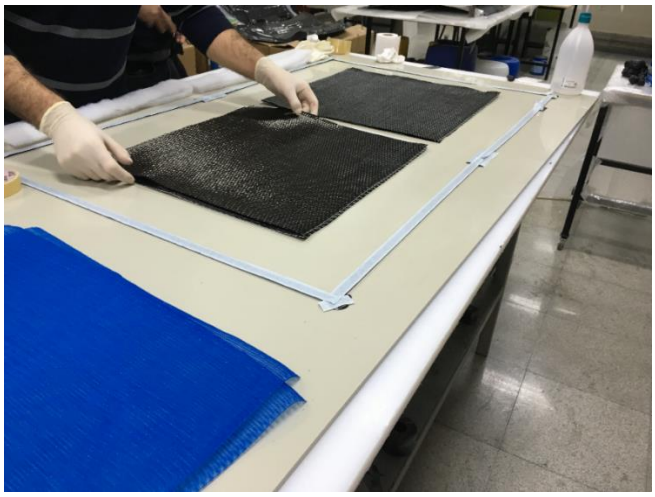

Figure 2.13. Initial step of vacuum infusion in composite fabrication

The next step is covering the area with the vacuum bag after laying the peel ply over reinforcement layers. The purpose of vacuum bag is to transport the resin into the fabric layers and it also helps to produce composite without air bubbles inside.

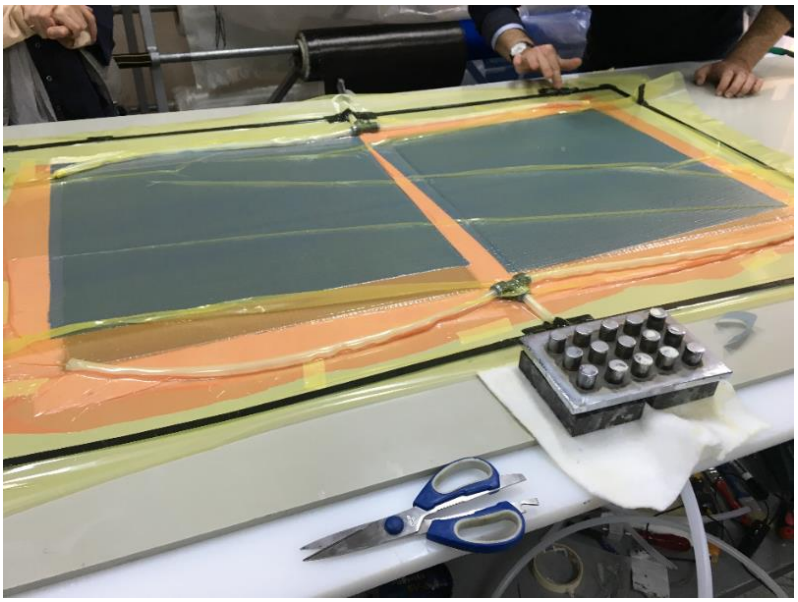

Figure 2.14. Composite part under vacuum (before resin infusion)

The last step is vacuuming the resin hardener mixture inside the layered fabrics. The vacuum pressure and resin distribution media help the resin flowing all over the surface uniformly (see figure 2.15). Vacuum pump controls the pressure inside the vacuum bag automatically to avoid any defects. When the infusion of resin is completely performed all over the surface, compressor can be turned off (around 3 or 4 hours later).

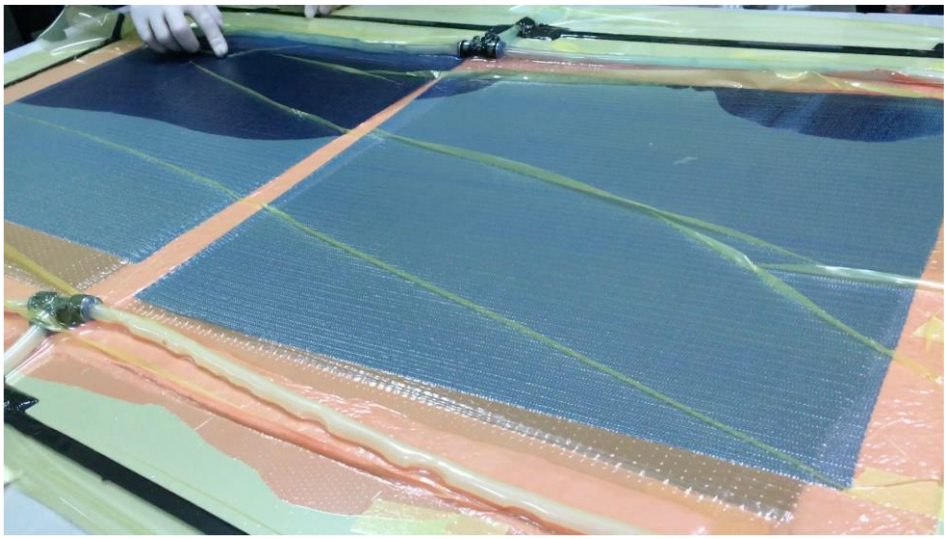

Figure 2.15. Resin flowing stage

Before embedding fiber Bragg grating sensors into the composite material, we realized two trial experiments with standard Single Mode Fiber (SMF). The reason for these trials is to understand the production process and to find a solution for the ingress points for the fiber optic cables. Due to the strong sticky tapers and additional peel ply

layers, it is hard to extract the material from table surface without breaking the fiber optical cables. In the first trial, we used standard cable macaron with 1.5 mm diameter as showed in figure 2.16 to give strength to fibers, but it caused an another problem for the vacuum bag. As it doesn't shrink the fiber in necessary amount, it caused air leakage from the bag. Thus, we looked for another solution for the ingress points of the fiber optical cables. We overcame this problem by using thin silicon tubes which were provided by University of Mons Electromagnetism and Telecommunication Department (UMONS) in Belgium.

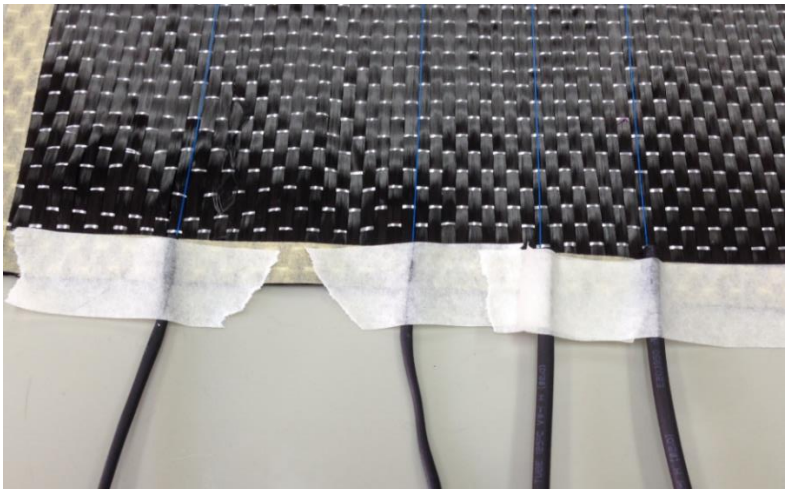

Figure 2.16. Cable macarons

2.3.2.2. FBG interrogation set-up

The first step is to connectorize the fiber Bragg grating sensors with the fusion fiber splicer. And second step is monitoring the FBG reflection spectrum with using a broadband laser source and optical spectrum analyzer (OSA). Figure 2.17 shows the basic set-up configuration.

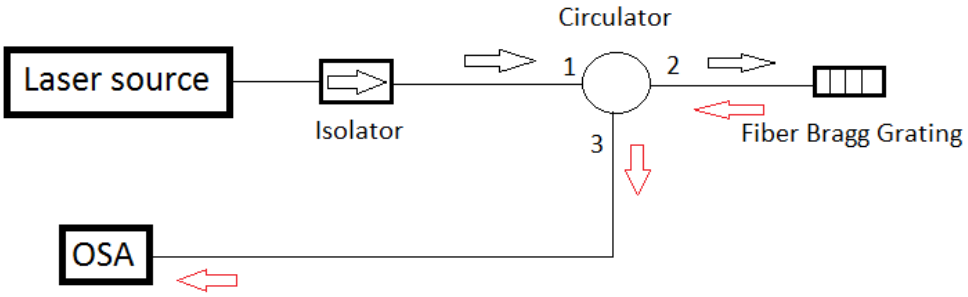

Figure 2.17. FBG interrogation set-up

The list of the used components is as follows;

- Broadband laser source (Thorlabs, ASE 730, Range 1530– 1610 nm)
- OSA (HP 71450B)
- Isolator
- Circulator (3-ports)
- Fiber Bragg gratings sensor (FBG), (Provided by UMONS)

Broadband laser source sends a broadband light within its range through the Isolator. It is used to prevent laser source from any back reflected light. Circulator is an optical component that transfers light between its terminals. In the figure 2.17, black colored arrows shows light propagation direction from source to FBG and red colored arrows shows the reflected light direction from FBG to OSA.

2.3.2.3. Embedding fiber Bragg grating sensors into the composite

As we have experienced by embedding standard SMF in preliminary experiments, fiber Bragg grating sensors were embedded successfully without having any breaks by protecting the ingress points with a thin silicon tubes. Figure 2.18 indicates our experimental set-up while resin flowing stage is continuing.

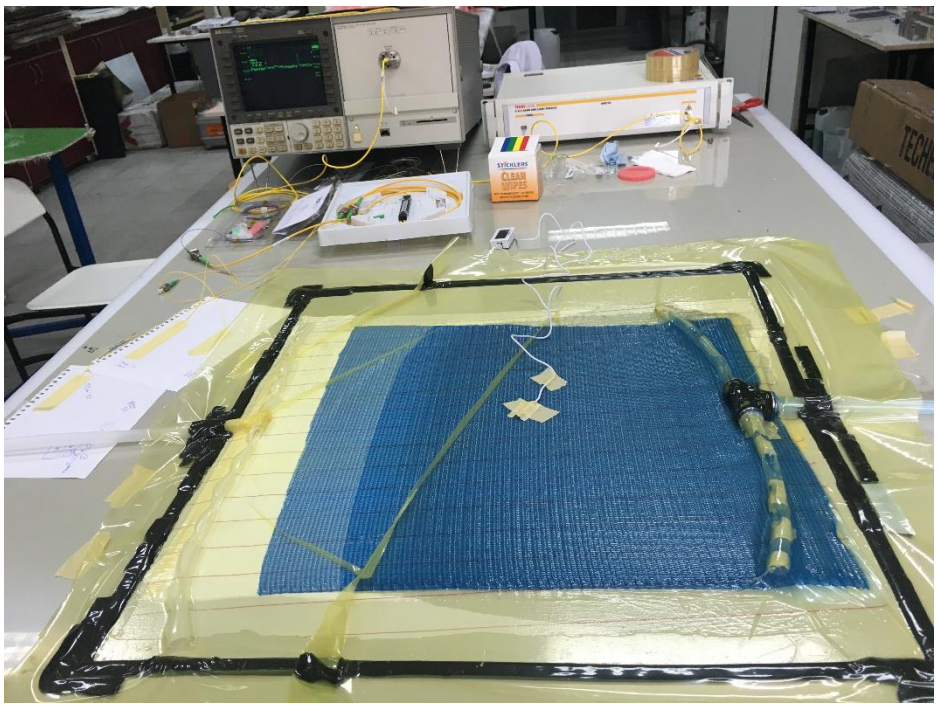

Figure 2.18. Resin flowing while FBG sensor measurements carrying out

The used resin type was Momentive Laminating Resin MGS L160 and hardener type is Momentive Hardener MGS H160. The mixture ratio was 65-35 percent respectively. This mixture has a curing cycle of 3 to 4 hours if production is realized in the room temperature. As a layer number we decided to use 4 layers of fabrics and placed the FBG sensors between the 2nd and 3rd layers.

While placing the fiber Bragg grating sensors, we covered one of the sensors with thin hermetic tube and used strong glue from the both sides to avoid resin infusion inside the hermetic tube. The reason for this process is to use this tubed FBG as a strain-free reference sensor. While the other FBG is exposed to both temperature and strain effects simultaneously, the tubed sensor gives only temperature information.

2.3.2.4. Results and discussions on monitoring of amplitude spectrum of FBG sensors during composite production

2.3.2.4.1. Sample 1

In the first sample, two FBG sensors were used to monitor the temperature and strain. Four carbon fiber reinforcement layers were used with dimension of 50 cm x 50 cm. Their Bragg wavelengths are 1548.73 nm and 1583 nm respectively. Figure 2.19 shows the Bragg wavelength evolutions for both sensors.

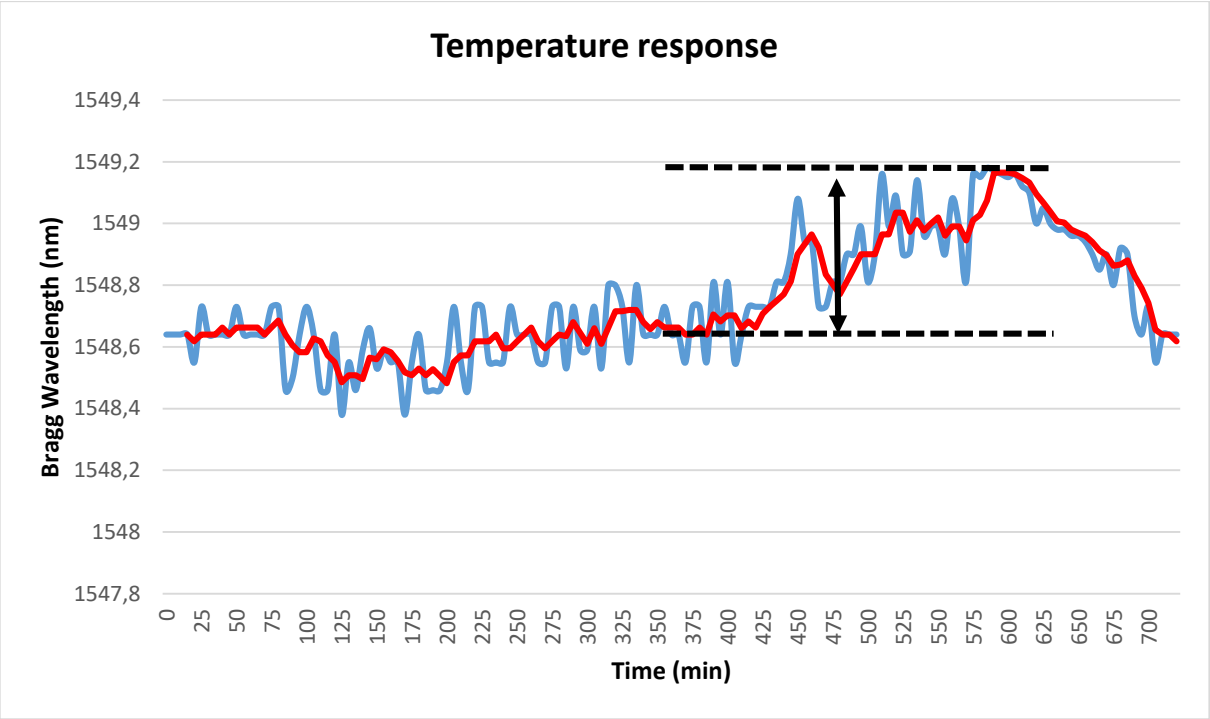

(a)

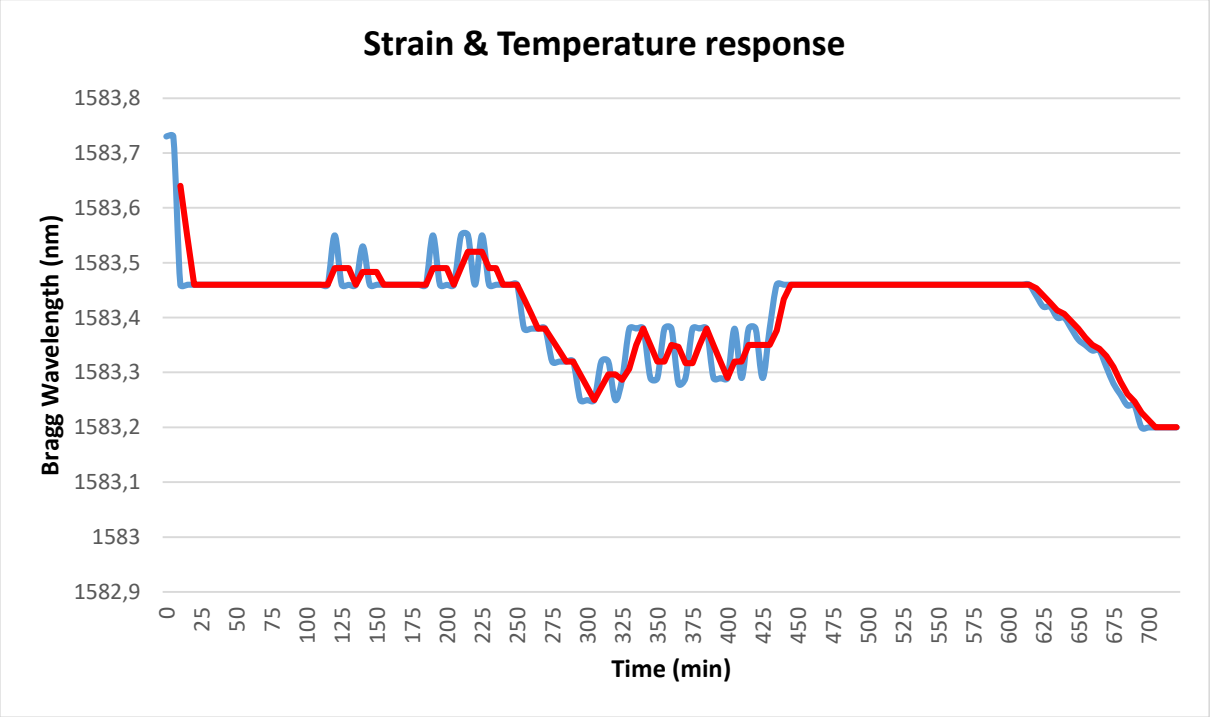

(b)

Figure 2.19. Bragg wavelength evolutions in time (sample 1)

In the figure 2.19 (a), we can observe that the curing happened around 400th minute since we have approximate 0.5 nm Brag wavelength shift in the temperature

sensor FBG. Temperature response of uniform FBG is 10 pm/C (see in section 2.1.1.2). Therefore, 500 pm wavelength shift results in 50 ^{0}C temperature change. It is expected order of magnitude considering of material type, size and number of layers (quite thin). When we look at the last value of Bragg wavelength in figure 2.19 (a), we can assume that the temperature sensor returns to its initial Bragg wavelength after curing process. It shows that hermetic tube prevented the temperature sensor from interacting with resin.

The strain sensors results in figure 2.19 (b) shows that there is a significant change in Bragg wavelength when FBG interacted with the resin in the resin flowing stage. Afterwards, we observe that the response is more or less constant during the process. At 250th minute wavelength started changing due to the state variation of the resin (from liquid phase to gel phase) while temperature sensor didn't show any reaction (it was inside the tube). Additionally, we can observe the residual strain effect when we look at the difference between the first and last values of Bragg wavelength. It started around 1583.4 nm and ended at 1583.2 nm that results in 200 pm difference. It corresponds to approximately 200 με.

2.3.2.4.2. Sample 2

For the second experiments, we decided to use four different FBGs. Two of them are for temperature sensing, placed in hermetic tubes and the other two FBGs are used to sense strain. In the second trial, we used four glass reinforced fiber layers (30 cm x 30 cm) so that we could be able to detect leakage points in the fiber network with fault locater device.

During the measurements, we observed that one of the temperature sensors reflection response was very noisy and lossy which makes it hard to see the reflection peak in OSA display. When we used the fault locator device, we observed that none of the FBGS was broken inside the composite but our splicing points were highly lossy. This must be the reason why we had lower aplitude reflection spectrum for the two FBGS. Additionally, one of the strain sensors reflection spectrum had very low amplitude due to the broadening of the spectrum. This lower amplitude signal was dominated by the noise in OSA.

This broadening of the pulses might be caused by two reasons:

- Birefringence of the fiber: Birefringence in optical fibers can be defined as refractive index difference (Δn) between orthogonal polarization modes (called the eigenmodes). The presence of asymmetries in the fiber section leads to Birefringence (broadening in reflection spectrum) [5].
- A non-uniform constraint: A non-uniform strain distribution along the FBG might result in deformed FBG reflection spectrum.

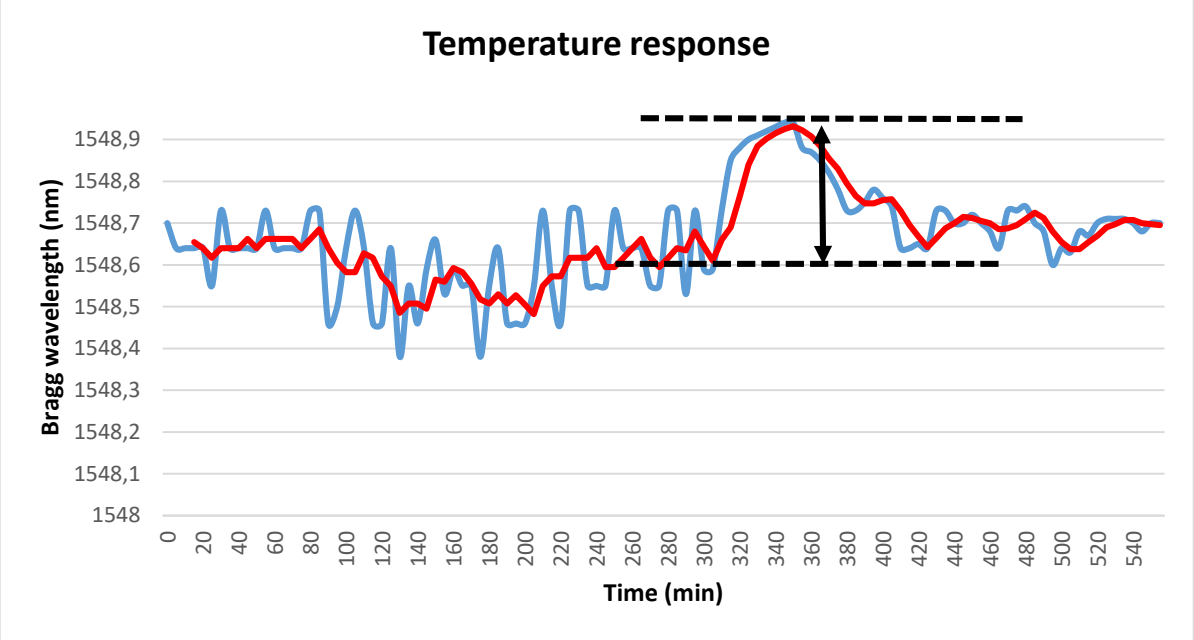

(a)

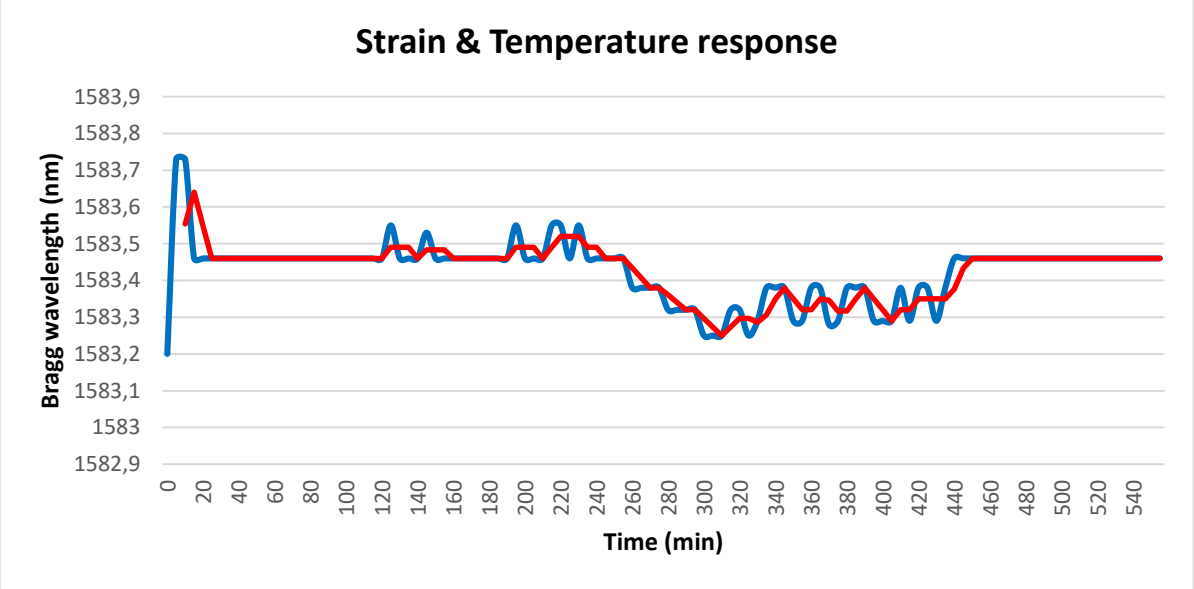

(b)

Figure 2.20. Bragg wavelength evolutions in time (sample 2)

In figure 2.20 (a), the Bragg wavelength of temperature sensor FBG started increasing at 300^{th} minute. There is an approximately 300 pm wavelength shift which corresponds to 30 ^{0}C. This temperature increase is due to the polymerization of the resin since it is an exothermic reaction. And like in the first experiment, we saw that it didn't affected by the residual strain effect as it is protected with hermetic tube.

As expected, significant residual strain in Fig 2.20 (b) was not observed due to the low temperature increase and low sized material. These slight variations may be dominated by optical spectrum analyzers noise. Indeed, we can say that there is no extreme strain on the FBGs to provoke a significant change in the Bragg wavelength that we could see. Thus, we can say that small sized materials produced by the vacuum infusion method has not big strain effects on FBGs.

In Fig 2.21, one can observe that temperature & strain sensor responses started changing due to the state variation of the resin (from liquid phase to gel phase) while temperature sensor response didn't show any significant change (it was inside the tube). The temperature sensor responses started changing at the time curing was started.

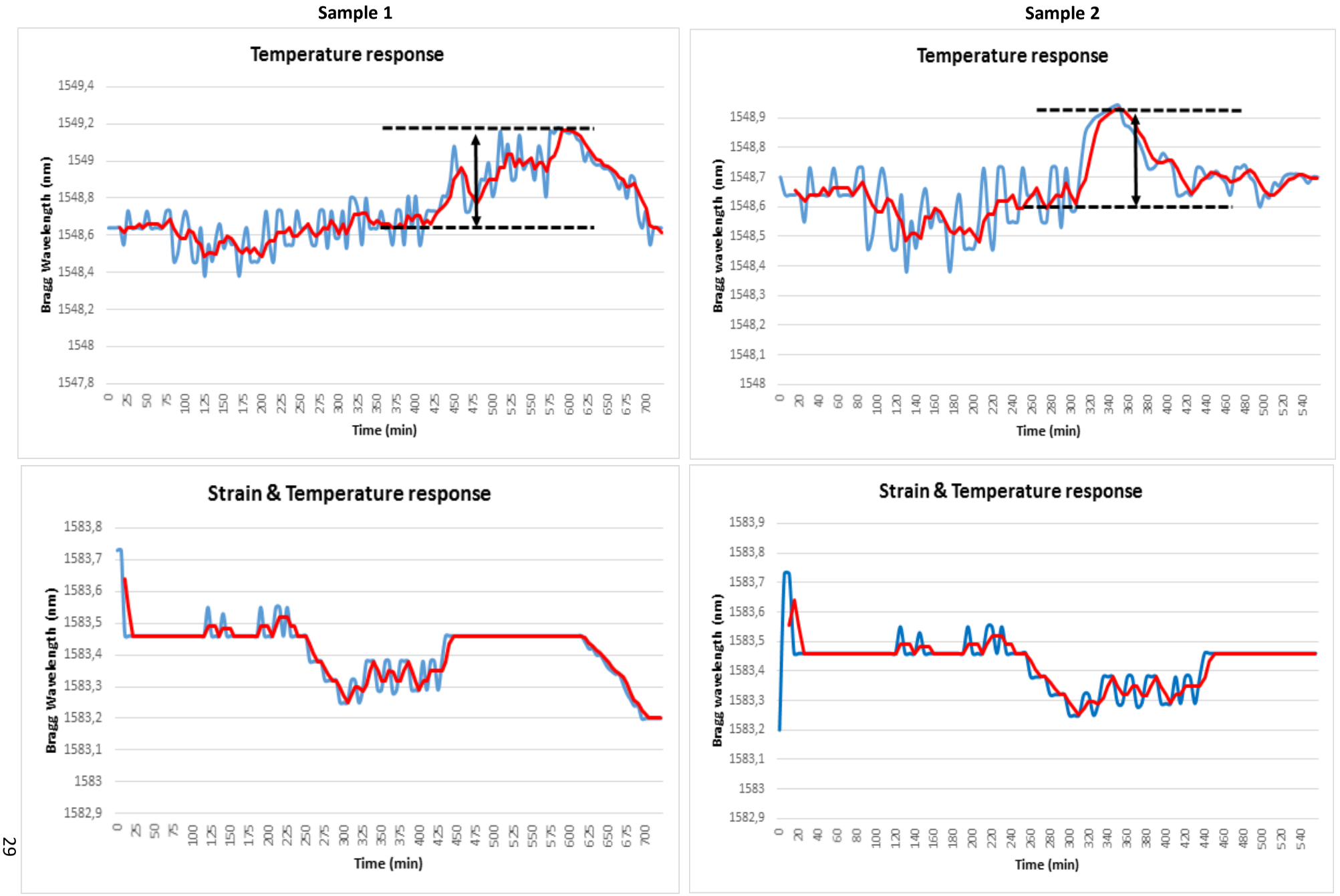

Figure 2.21. Comparison of FBG wavelength shifts

2.4. Conclusion

This chapter summarized two different fiber optical sensor implementations used during the production stages of composite materials. At first, Fresnel reflection based sensor was realized to measure the refractive index changes of resin and hardener mixture by measuring reflection values and calculating refractive indices by using equations 2.9 and 2.10. And in the next step, fiber Bragg grating sensor applications were realized for process monitoring of composite materials in the department of Mechanical Engineering at IZTECH. These experiments gave us more insight about FBG sensors implementation and composite material production.

CHAPTER 3

IMPLEMENTATION OF FIBER CAVITY RING-DOWN LOOP INTERROGATED BY OPTICAL TIME DOMAIN REFLECTOMETRY

3.1. Fiber cavity ring-down loop concept

Fiber cavity ring-down (CRD) spectroscopy technique is a quite preferred sensor technology in chemical and physical analysis [15]. With significant amount of researches accomplished in this area, a variety of configurations were presented during the last decade based on the same working principle [16]. Real time measurement, remote sensing and easy usage of this technology make fiber cavity ring-down loop a more attractive method [17]. CRD technique can be implemented to measure different physical parameters such as temperature [18], strain [19] and pressure [20].

Typical CRD loop basically uses a fiber loop to create a resonant cavity with a sensing head placed inside the fiber loop [16]. This resonant cavity is constructed by placing two optical fiber couplers into a fiber network as indicated in figure 3.1. The flexibility of this application is that it enables the usage of variety of sensing components (represented as sensing head in figure 3.1) such as fiber Bragg gratings, long period gratings and etched fibers [16]. The couplers in this representation help to keep the light travelling inside the loop until the light power decreases to low levels.

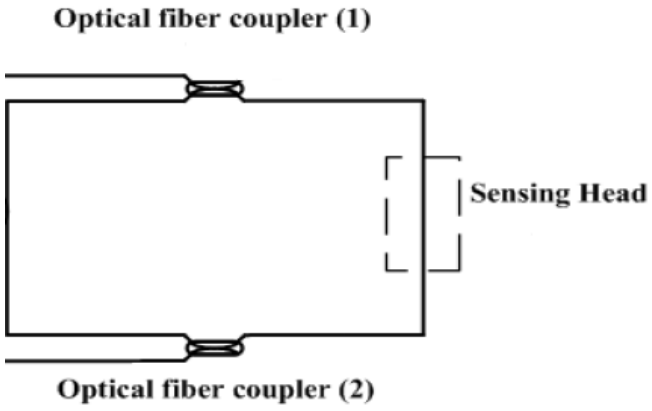

Figure 3.1. Resonant cavity created with fiber loop [17]

The operation principle of fiber CRD technique is basically to generate a loop so that an optical pulse can make several turns inside the fiber loop. The purpose of the first coupler is to send the pulse into the loop. Each time the pulse is making a complete cycle through the loop, the second coupler extracts certain portion of the incoming pulse toward the detection unit (to measure the light power).

While light is traveling through the loop, it is exposed to the fiber attenuation, the insertion losses of couplers, and the attenuation imposed by the sensor head. This means that pulse will start decaying slowly after each turn in the loop.

Conventional fiber CRD techniques in the previous studies use an optical pulse source to send the pulse into the loop and employs a photo-detector cascading with an oscilloscope to detect the output signals intensity as shown in figure 3.2 [16] [17].

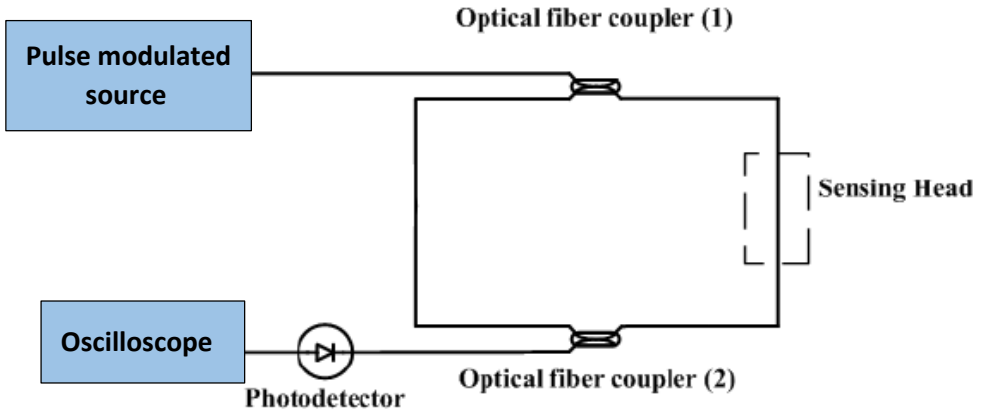

Figure 3.2. Conventional fiber CRD method

However, this configuration requires more components (fast and expensive photodetector and oscilloscope) to establish the interrogation set-up.

What we propose in this thesis is to use an Optical Time-Domain Reflectometry (OTDR) and a simple fiber circulator component to send, receive and analyze the pulses by using only one device. The proposed method is much more simple, robust and flexible compared to previous configurations.

3.2. Proposed method to interrogate fiber CRD loop

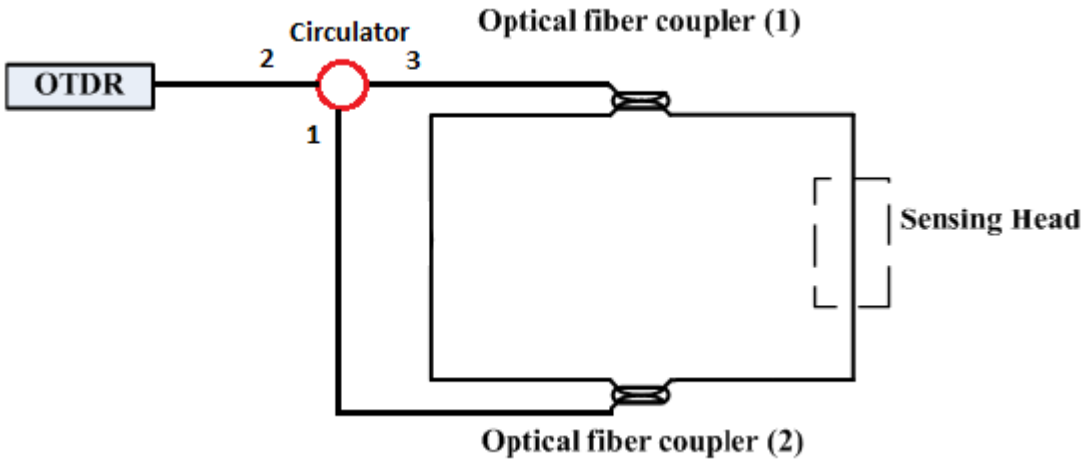

Figure 3.3. Proposed fiber CRD method

Figure 3.3 demonstrates our proposed fiber cavity ring-down loop method by using OTDR as a source and detecting unit with the help of a circulator. Circulator is a component that has three ports and it is connected such a way that it sends the light from port 1 to port 2 and from port 2 to port 3 (i.e the circulator blocks the signal in the counter clockwise direction). Therefore, it helps us to prevent from undesired back reflected lights as we focused on the light travelling through the loop.

The basic working principle of this set-up can be explained step by step as follows:

1) OTDR sends a light pulse at 1550 nm with a specific pulse width through the circulator (port 2→port 3) to the coupler 1 (3-dB coupler).
2) When the pulse arrives at the coupler 2, 10% percent of the pulse is sent to the OTDR by passing through the circulator (port 1→port 2) where %90 percent of the pulse continues its way through the coupler 1.
3) %90 percent of the pulse follows the loop by passing through the coupler 1 and coupler 2 and again %10 percent of the remaining pulse is sent to the OTDR via circulator ports.
4) These second and third steps continue until the pulse power decreases to very low values.

These several turns within the loop result in a signal decaying in time due to the losses and attenuations which makes the fiber CRD loop a perfect tool to use in sensor applications [8]. This decay can be demonstrated with an example in figure 3.4

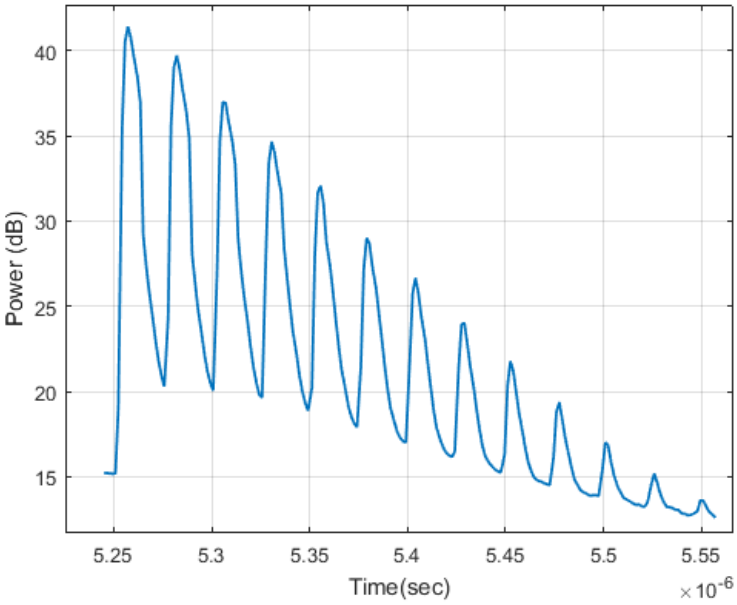

Figure 3.4. Cavity ring-down decay in time

3.2.1. Optical time-domain reflectometry (OTDR)

Optical time domain reflectometry (OTDR) is a well-known reflectometry technique for the characterization of fiber optical networks. The basic operation principle of this reflectometry technique is the measurement of the Rayleigh backscattered signal when an optical pulse is launched into the fiber [21].

The working principle of an OTDR is as follows: at time t = 0, a laser launches an optical pulse into the fiber link. When this pulse propagates along the fiber, it is attenuated and continuously scattered in all direction via the Rayleigh scattering process. Some portion of this scattered signal is captured by the fiber and propagates back towards the OTDR. Figure 3.5 simply shows this phenomenon [21].

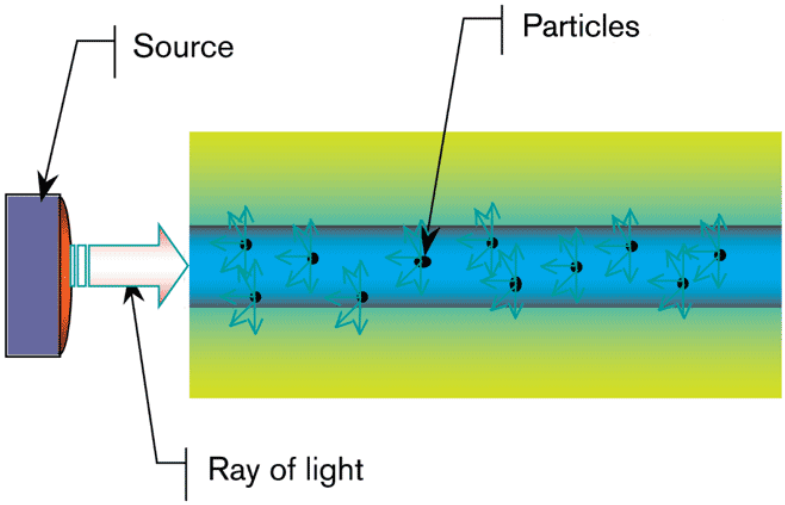

Figure 3.5. Rayleigh backscattered light [22]

Another type of reflection in OTDR is the Fresnel reflection. It actually helps us to detect all the physical events along the fiber link. When the light wave hits an abrupt change in refractive index such as from glass to air, a higher amount of light is reflected back creating Fresnel reflection [21]. Examples of such reflective events are connectors, mechanical splices, fiber breaks, bulkheads or opened connectors. Figure 3.6 below illustrates different events that create Fresnel reflections.

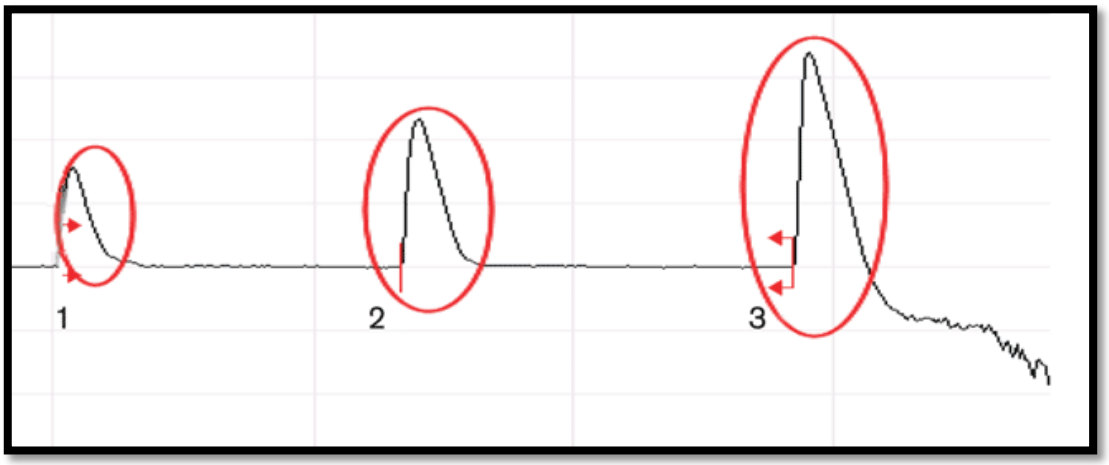

Figure 3.6. Fresnel reflections created by (1) mechanical splice, (2) bulkhead and (3) opened connection [22]

Fresnel reflections lead to another significant OTDR specification called *dead zones*. There are two types of dead zones (event and attenuation). Both of them are originated from Fresnel reflections. A typical definition of dead zone is the length of time

during which the photo-detector of OTDR is temporary blinded due to a high amount of reflected light, until it recovers and can detect light again [22].

In the OTDR measurements, time is converted into distance domain by simply calculating the speed of light in fiber; therefore, dead zone is expressed in distance-domain (m) and it is related to the pulse width of the OTDR signal [23]. Thus, pulse width of the signal is another parameter to be taken into account during the experiments. Lower pulse width provides us with better spatial resolution at the expense of shorter measurement range (due to lower power). Figure 3.7 shows the effect of pulse width on the dead zone more clearly.

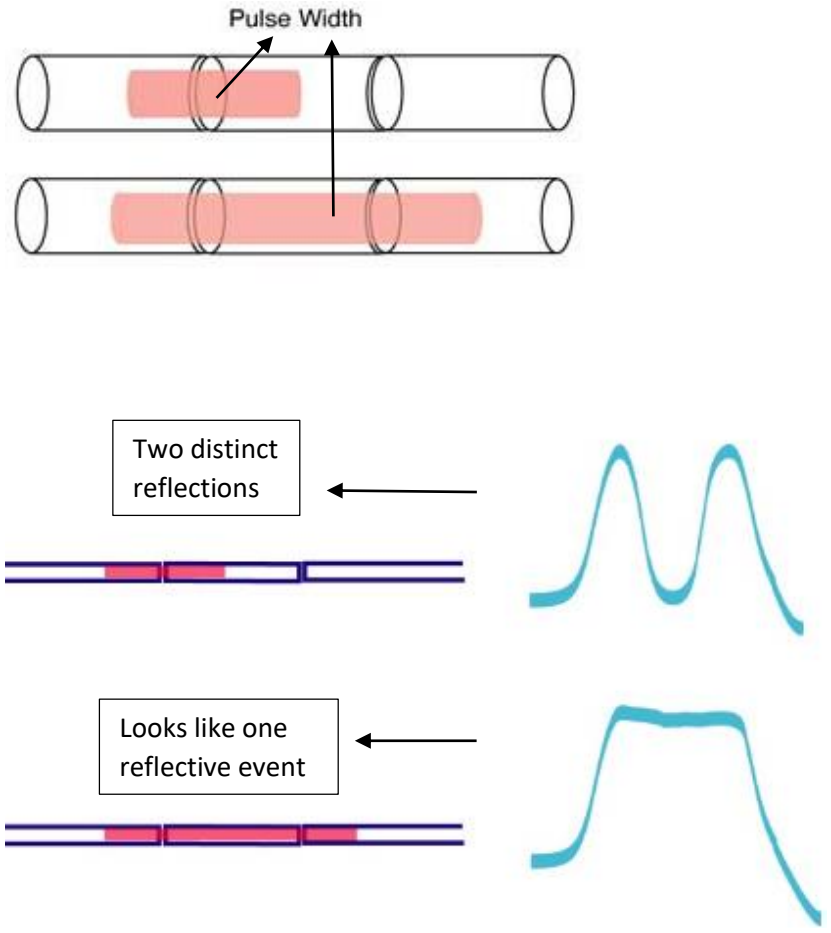

Figure 3.7. Pulse width & dead zone relation [23]

OTDR measurements typically are based on monitoring the backscattered and back reflected portions of the pulse, not the pulse itself. It should be noted that, in our work, the OTDR is used in an original way. That is to say, by connecting the OTDR and fiber loop by the way of a circulator, the pulses sent by the OTDR making several turns within the loop are detected and analyzed.

3.2.2. Theory of fiber cavity ring-down loop interrogated by OTDR

The power of the pulse at time t is related to the initial power (P_0) of the pulse as [24];

$$P = P_0 \cdot e^{-\left(\frac{A \cdot c \cdot t}{n \cdot L}\right)} \qquad (3.1)$$

In Equation (3.1), A is the total transmission loss of the light in the loop, c is the speed of light, n is the refractive index of the fiber, and L is the length of the fiber loop [12].

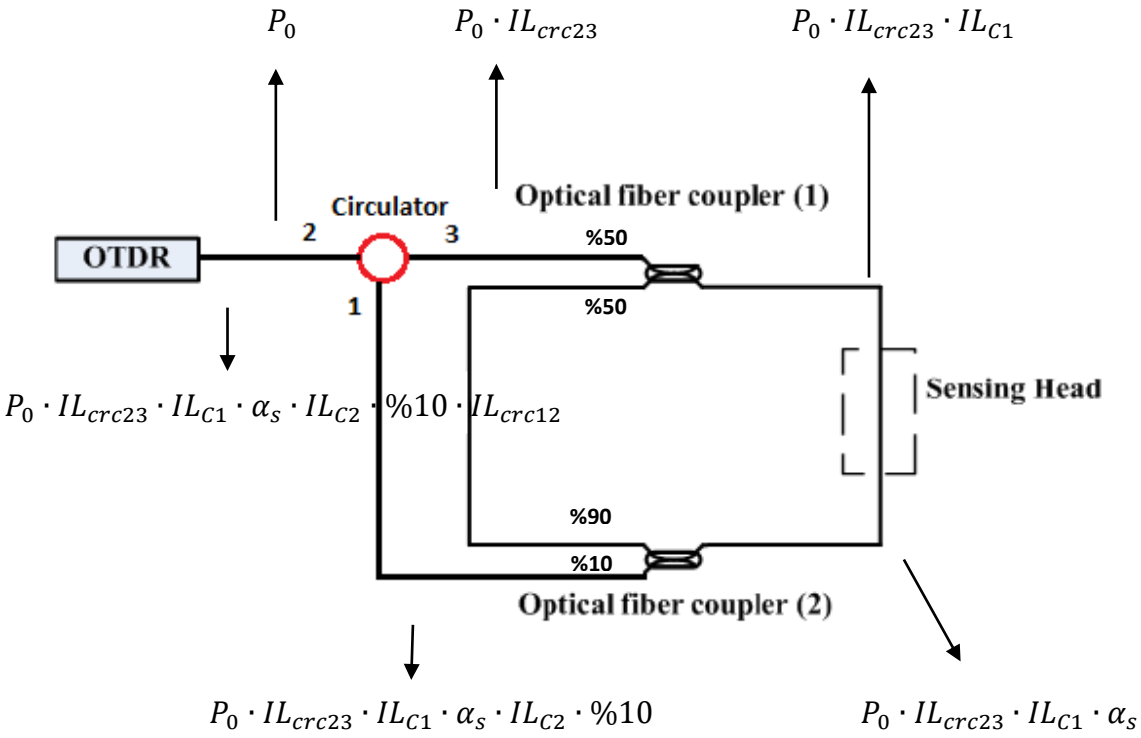

Figure 3.8. Pulse travel

Above equations show the evolution of the signal when it passes each component. P_0 is the initial launched pulse power, and IL_{crc}, IL_{C1} and IL_{C2} are for the insertion losses of circulator, coupler 1 and coupler 2 and α_s stands for the attenuation factor of the sensor head.

Coupler 2 splits the incoming signal within the ratio %90 - %10. As it is aimed to create a cavity by letting the light travel inside the loop, it is logical to keep the higher portion inside loop and send the lower amount of portion to the OTDR.

Equation 3.2 is the formulation of the first pulse arriving at the OTDR detector. Starting from the second round, there will be series of pulses arriving at the OTDR detector and indicated by S_{OTDR} in equation (3.3).

$$P_0 \cdot IL_{crc23} \cdot IL_{C1} \cdot \alpha_s \cdot IL_{C2} \cdot \%10 \cdot IL_{crc12} \qquad (3.2)$$

$$S_{OTDR} = P_0 \cdot IL_{crc23} \cdot IL_{C1} \cdot \alpha \cdot IL_{C2} \cdot \%10 \cdot IL_{crc12} \cdot (IL_{C1} \cdot \alpha \cdot IL_{C2} \cdot \%90)^k$$

$$k = 0,1,2 \ldots \qquad (3.3)$$

OTDR converts this signal into dB domain by taking the logarithm of it. OTDR also divides the signal into two as in the usual configuration, the signal arriving to OTDR makes a round trip.

As shown in equation (3.1) the signal arriving to the OTDR is expected to have an exponential decay [16] [17]. This decay appears as a linear slope on the OTDR display since it takes logarithm of the detected signal as explained above.

The sensor head produces diverse attenuation values with factor α_s [24]. This attenuation level shows linear relation with the slope of fitted line which is produced by the decaying peak points of the signal as in figure 3.9. The relation between attenuation value and slope makes fiber CRD loop technology perfect candidate for sensor applications.

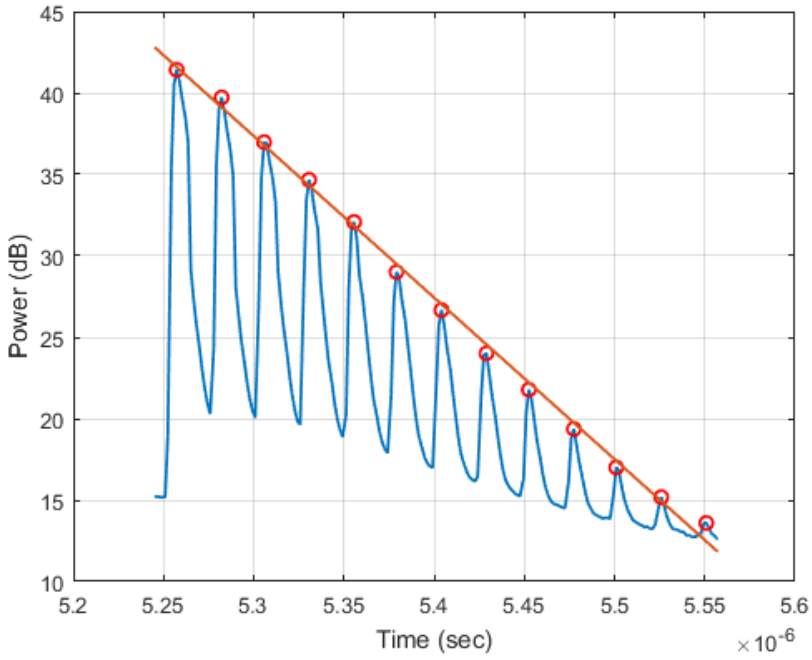

Figure 3.9. Fitted line for the peak points of the signal

3.3. Experimental set-up

3.3.1. Fiber CRD loop set-up

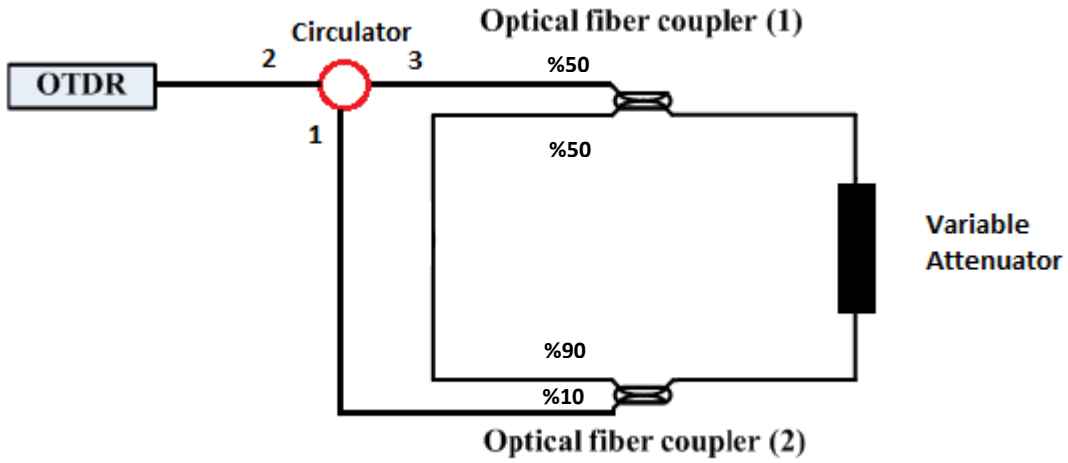

Figure 3.10. Fiber CRD loop set-up

As the operating principle of fiber CRD loop explained in detail within the previous sections, experimental set-up was realized in the framework of this thesis. Fig 3.10 demonstrates the block diagram of the experimental set-up.

The list of the used components is as follows;

- OTDR (EXFO FTB 7300E SM OTDR module on FTB-500 Modular Mainframe), (operating at 1550 nm & 1625 nm)
- Circulator 3-ports
- Coupler 1 (50:50), Coupler 2 (10:90)
- Variable Attenuator (Thorlabs VOA50-APC) (Range 1.5-50 dB)

OTDR sends pulses (wavelength 1550 nm) at a desired pulse width and then receives the returning pulses transferred via the circulator. For each measurement, the ASCII files containing the OTDR parameters and measured values of power versus position are provided by the user-friendly interface of the OTDR. These ASCII files are then processed by our custom MATLAB code in order to extract the sensor response from the OTDR trace.

Circulator is the connection between OTDR and fiber loop. With the help of the circulator, pulses sent by the OTDR are not only injected into the loop, but also directed back into the OTDR after traveling in the loop.

Couplers are used to create a cavity to keep the light inside the loop as long as the sufficient light power still remains. Division range of the both couplers directly influences the number of turns inside the loop since they transmit only a certain portion of the light to the loop and to the OTDR after each turn. Two couplers with the coupling ratios of 50:50 and 10:90 are used in our experiments simply because of their availability in the laboratory (two couplers of 10:90 would have been a better choice to obtain a greater time constant).

The purpose of variable attenuator is to generate diverse attenuation levels inside the loop in order to mimic a sensor response.

However, in practice changing the attenuation level with a regular interval in a controlled manner is a challenging issue due to the type of the attenuator we have in hand. Indeed, this device introduces different attenuation levels by simply turning the screw mounted on it. Therefore, it is needed to calibrate the device by measuring the attenuation levels induced by different screw positions applied on it. We obtained this calibration characteristics by the way of another set-up that we used in parallel to the main experimental set-up as described in the following section.

3.3.2. Attenuation level calibrating set-up

Below schematic displays the set-up to measure the attenuation levels introduced by variable attenuator at different adjustment screw positions.

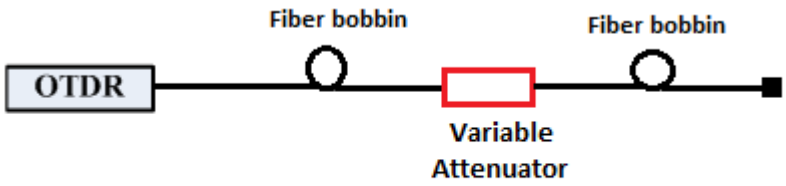

Figure 3.11. Attenuation level calibrating set-up

In this set-up, the variable attenuator is placed between two bobbins with the length of 1070 m and 1120 m to observe a power level drop at the attenuator's position. The approach to extract the attenuation level is demonstrated in the figure 3.12. The power drop (in dB) corresponding to the loss inserted by the attenuator is represented as the difference between two dashed lines (before and the after the attenuator). This loss is equal to the sum of the imposed attenuation value and the insertion loss of the device (≤1.5 dB).

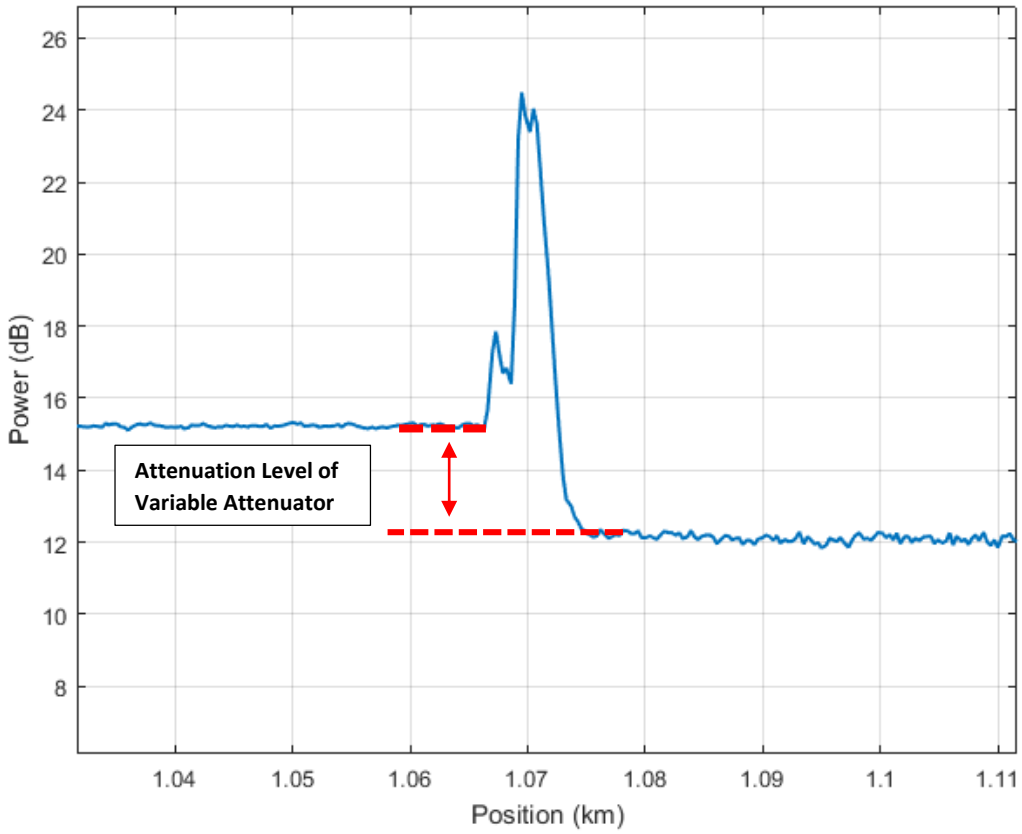

Figure 3.12. Attenuation level detection approach

These experiments require a high sensitivity and stable work bench for each trial since the same variable attenuator is placed into the fiber CRD loop after disconnecting it from attenuation detection set-up. After at least ten successive trials of measurements, precision value for variable attenuator is measured as ± 0.18 dB.

3.4. Results and Discussion

In this part of the thesis, we present the measurement results followed by the related comments and discussions. Firstly, we explain the selection process of the OTDR parameters convenient to our sensor implementation. Then, we determine the attenuation interval to be used in the measurements. Afterwards, we test our proposed set-up to interrogate the attenuation interval applied in the loop as a sensor head. Lastly, test results are discussed.

3.4.1. Determining convenient pulse width of OTDR

OTDR device provides us the flexibility of selecting the pulse width (W) to be used as a test signal. Thus, it is needed to study the behavior of the pulse width over OTDR signal before calibrating the fiber cavity ring-down loop.

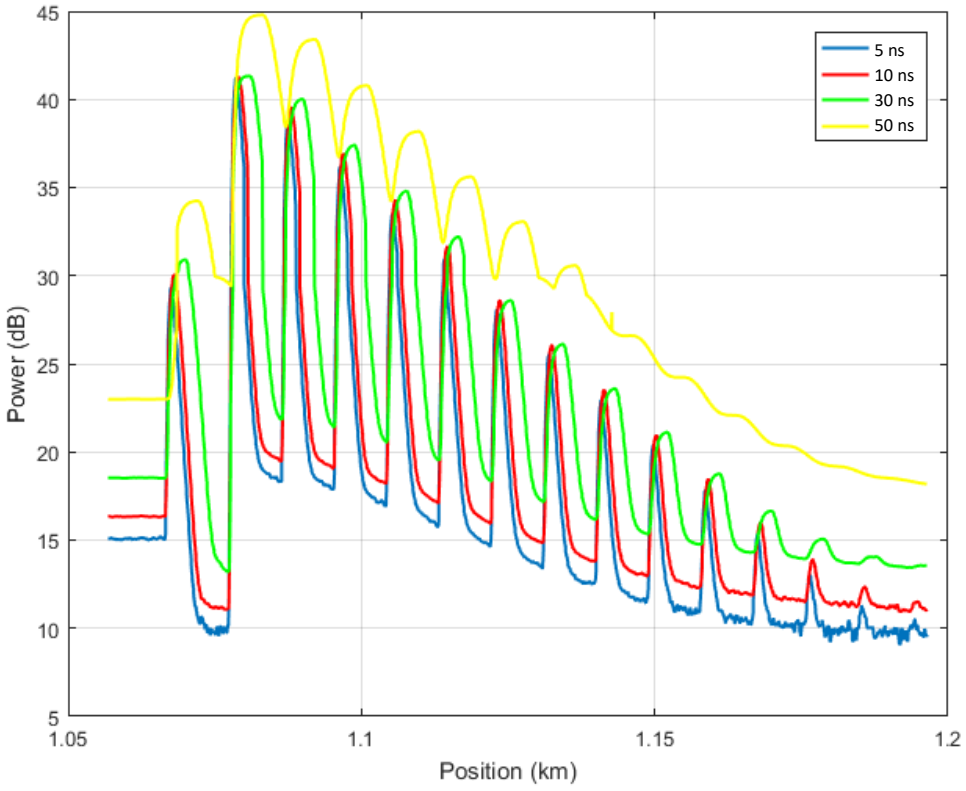

Figure 3.13. Cavity ring-down traces for diverse pulse widths

Four different cavity ring-down traces in figure 3.13 show the effect of the pulse width in the OTDR trace. The first apparent difference is the change in the power levels of the launched pulses. The wider the pulse, the higher the power level of the test signal, in the expense of spatial resolution. A typical dead zone value is 8m for a pulse width of 10ns [9]. Therefore, the length of the cavity ring-down is arranged as 18 m to prevent the signal from dead zone effect as much as possible during tests.

In order to decide the pulse width in our measurements, we have to consider the tradeoff between spatial resolution and dynamic range. The former provides the ease of distinguishing between successive peaks in the pulse series. The latter on the other hand, is of interest for remote sensing applications where longer distances are involved.

The distances in our experiment set-up is in the order of a few km. Therefore, we decided to use the shortest pulse width (5 ns) provided by our OTDR in order to obtain the better spatial resolution necessary to resolve the peaks from the cavity.

3.4.2. Attenuation level measurements and discussion

Six different attenuation levels imposed by the variable attenuator are displayed in figure 3.14 (W=5 ns, averaging time=25 sec, measurement range=5 km).

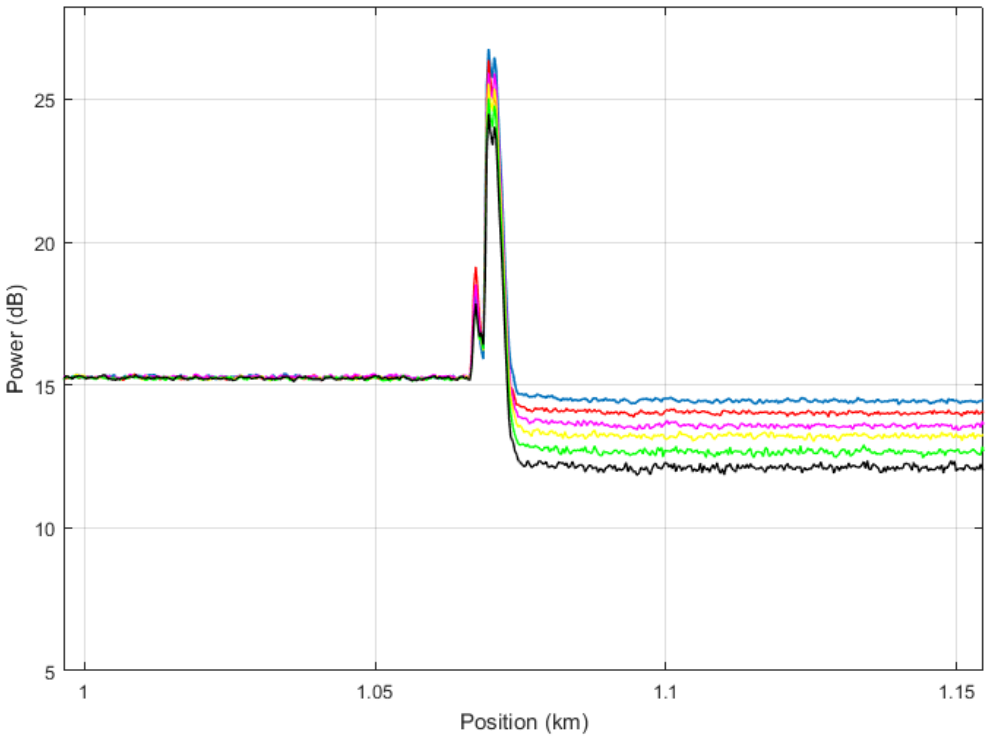

Figure 3.14. Different attenuation levels

As already explained in section 3.3.2, the amount of applied attenuations is obtained on the OTDR trace as a power level difference in dB between two ports of the variable attenuator. Table 3.1 indicates the measured attenuation values from these tests.

Table 3.1. Measured attenuation levels

Screw position	Attenuation Level (dB)
1	0.68
2	1.25
3	1.56
4	1.93
5	2.35
6	3.32

These measured attenuation levels are used to compare the decaying line slopes of the fiber CRD loops signals peaks. As already mentioned in section 3.3.1, the purpose of using variable attenuator is to interrogate the sensor response by using the fiber CRD loop technology. A comprehensive discussion about the influence of these attenuations will be held in the next sections.

3.4.3. Cavity ring-down interrogation of the sensor head for diverse attenuation levels

After detecting each attenuation level of the variable attenuator, it is connected to the fiber cavity ring-down loop as a sensor head.

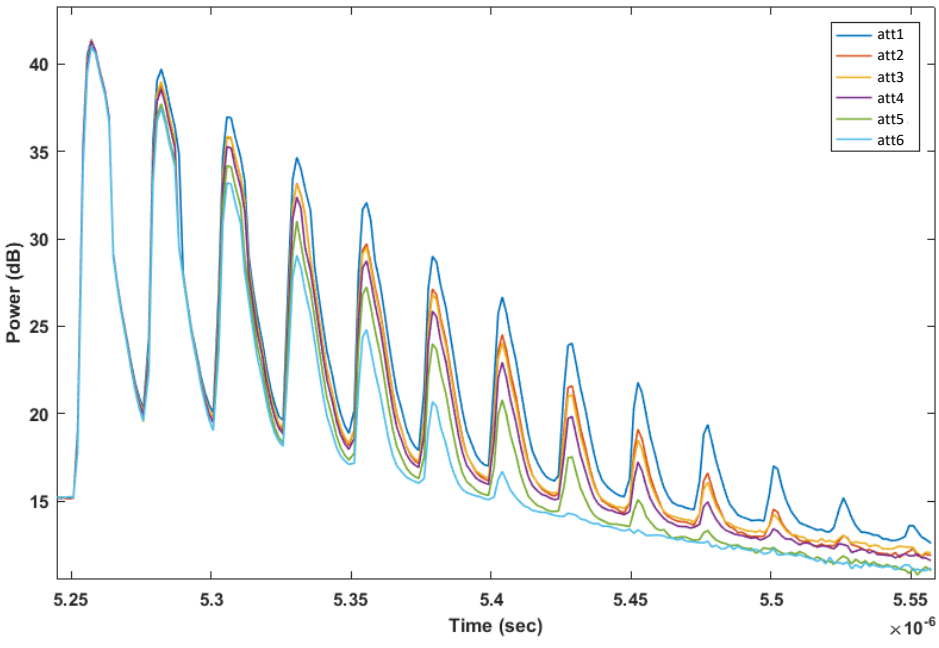

Figure 3.15. Fiber cavity ring-down traces for different attenuation values

Figure 3.15 illustrates six different OTDR traces obtained for different attenuation values listed in Table 3.1. A total number of 13 reflection peaks can be observable when an attenuation of 0.68 dB is inserted in the loop, whereas only 7 reflection peaks are distinguishable at an attenuation of 3.32 dB. This obvious result is due to the fact that, for the latter case, the pulse experience more attenuation during each travel in the loop, leading to sharper fitting line with a higher slope.

The next step is to extract the peak points from the OTDR trace taken for each attenuation level and to construct an appropriate fit line for those peak points (by the way of simple signal manipulation using MATLAB). An example fit line obtained for, 0.68 dB of attenuation is shown in figure 3.16.

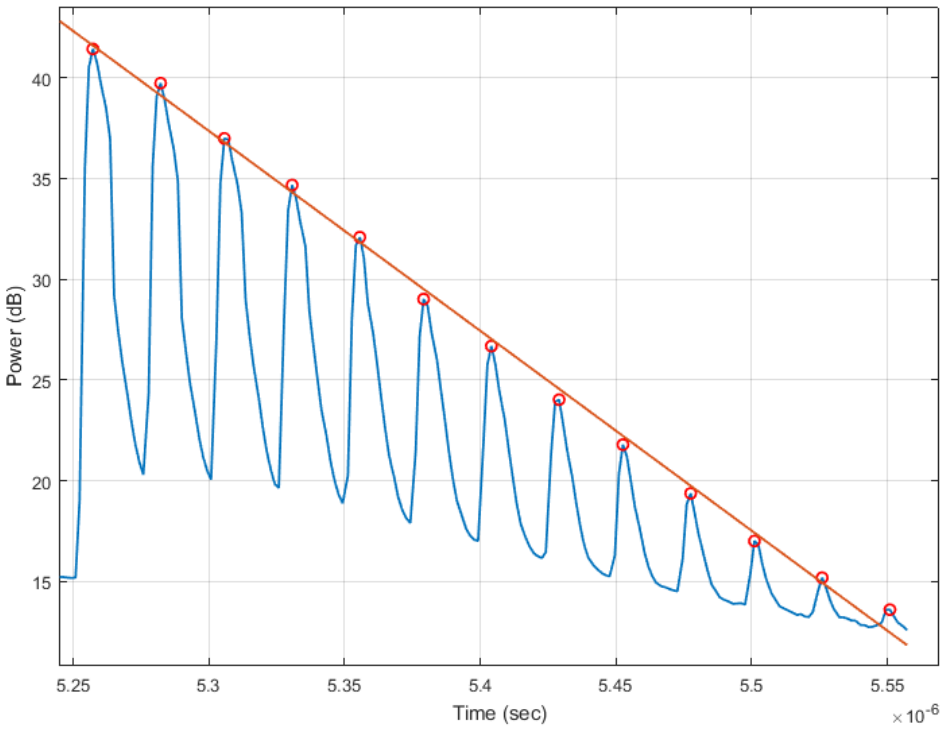

Figure 3.16. Decay fit line for the sample and with 0.68 dB of attenuation (W=5 ns)

In the conventional fiber cavity ring-down configurations reported in the previous literature, the interrogation signal exhibits an exponential decay (cf eq 3.1). In our proposed approach, OTDR takes the logarithm of the signal and yields linearly decreasing signal. Using OTDR to monitor the cavity ring-down loop not only decreases the number

of components in set-up but also provides us with user-friendly interface to process data under MATLAB for further studies.

Aforementioned test procedure has been repeated for all the six attenuation levels and the corresponding fit lines have been constructed. Figure 3.17 demonstrates the comparison between these data fit lines, on the same graph in the form of power versus time.

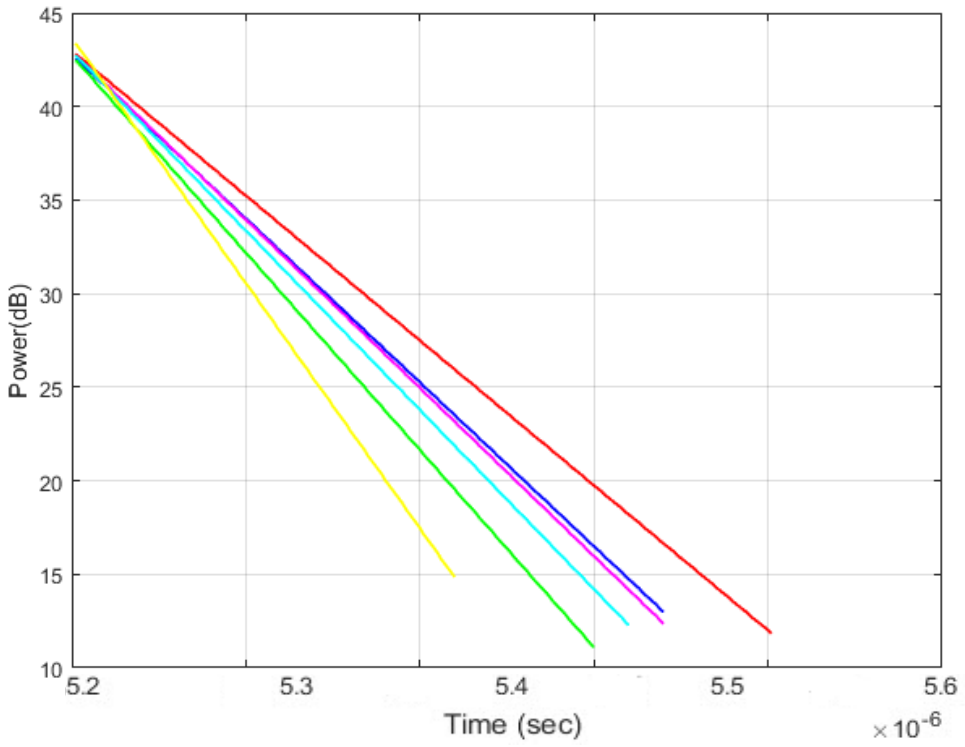

Figure 3.17. Constructed fit lines for six different attenuation levels

The absolute values of slopes for each line are listed in table 3.2. One can observe that, higher attenuation level in the loop means sharper fit line (see in figure 3.17).

Table 3.2. Fit line slopes corresponding each attenuation level

Screw position	Attenuation Level (dB)	Slopes (dB/sec)
1	0.68	$0.992 \cdot 10^8$
2	1.25	$1.122 \cdot 10^8$
3	1.56	$1.151 \cdot 10^8$
4	1.93	$1.227 \cdot 10^8$
5	2.35	$1.350 \cdot 10^8$
6	3.32	$1.680 \cdot 10^8$

Finally, the response of our sensor interrogation approach is characterized in figure 3.18 where the slopes of the fitted lines is represented as a function of attenuation levels. The linear response (with ±0.18 dB precision) observed in this calibration work successfully demonstrates the feasibility of using OTDR-based fiber CRD technique for as a sensor interrogation tool.

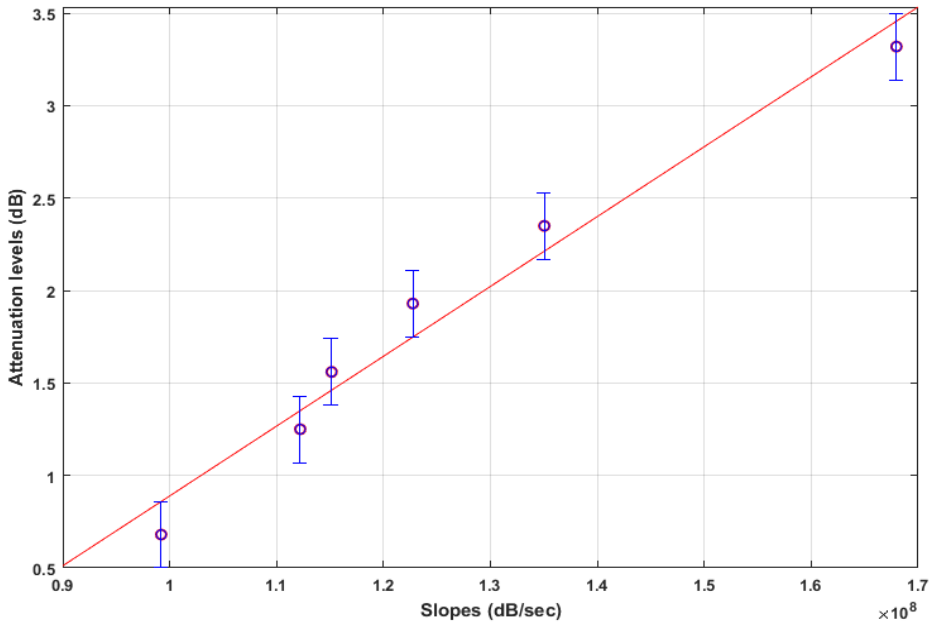

Figure 3.18. Linear response of the proposed sensor: relation between the cavity decay time and the attenuation level of the sensor head

As attenuation value increases, there is an increase in the absolute value of the slope. In the envisaged application, these attenuation will be caused by physical parameters such as strain, pressure, or temperature.

3.5. Conclusion

We experimentally demonstrated a novel sensor interrogation approach based on fiber cavity ring-down and OTDR technologies. Using OTDR as an interrogation unit makes this technology more simple and convenient for variety sensor applications. Instead of using pulse modulator setup, oscilloscope and fast photo-detector, OTDR can manage sending and receiving the light pulse on itself.

CHAPTER 4

CONCLUSION

In parallel to the aims of productivity and security, a major concern has been becoming increasingly important for today's science and technology: reduced energy consumption and, consequently, CO2 emissions. For many industrial sectors, such as transportation, aerospace, and renewable energy (wind turbines), this concern can be addressed by lightening the structure of mechanical pieces. It is made possible by replacing metallic part by composite materials while keeping intact the important requirements of mechanical performance of the final product. However, the behavior of composite materials under loading is different from metals and measuring strain distribution and loads on the composite materials results in improved performance and safety together with reduced costs in many ways. Residual stresses appearing during fabrication process (curing) is of particular interest for composite materials as they may weaken the structure and increase the risk of sudden breakage. Fiber-reinforced composites are indeed fragile in out-plane- direction because of their anisotropic nature and can be damaged by excessive transverse loads. Many groups have been working to develop novel technologies based on Fiber Optic Sensors (FOS) for monitoring production steps and strain distribution of the composite structures.

In this context, the aim of this thesis is to demonstrate the fiber optical sensor implementation on composite materials and develop new sensor interrogation approach to be applied in this area.

Second chapter of this thesis starts with presenting fiber optical sensor classifications by focusing on fiber Bragg gratings and Fresnel reflection based sensors. Theoretical principles of these sensor technologies are explained in details. And in the following, the state of the art on composite materials is expressed. It covers their advantages compared to conventional materials, structural components and two manufacture techniques (resin transfer molding and vacuum-assisted resin infusion).

The first experimental study in this chapter is done to monitor the curing process of resin and hardener mixture with the help of Fresnel reflection based sensor approach.

To do so, OTDR is used to measure the Fresnel reflections at the intersection of two medium (fiber end – resin hardener mixture). By using these measured values in indicated formulas, refractive index profile for curing process is extracted and discussed.

Afterwards, experiments to embed standard fiber optical cable to the composite material is realized as a preliminary step before embedding FBGs. The purpose of this trial is to come up with a solution to protect fiber ingress points (thin silicon tubes). In the following of these works, FBG sensors are embedded into composite material for process monitoring of composite materials. Tunable laser source (TLS) is used to launch a broad band light signal. Optical spectrum analyzer (OSA) is used to observe the reflection spectrum of fiber Bragg gratings. The experiments carried out in this study and the measurement results are discussed at the end of chapter three.

A theoretical model and experimental set-up to monitor the sensor response of fiber CRD loop were introduced in chapter three. A variable attenuator was used to mimic the effect of sensor head in CRD loop. OTDR was the interrogation unit for both launching and receiving the optical pulse through the circulator device. Using the OTDR in the original configuration explored in this chapter brings many advantages such as lower cost, simplicity, robustness, and higher tolerance to external temperature.

4.1. Perspectives

Several application areas related to the experiments demonstrated in this thesis can be foreseen as future research topics:

● Embedding these FBG sensors into composite materials successfully opens a door for *structural health monitoring (SHM)* of composite materials. Structural health monitoring is described as the process of implementing a damage identification strategy for aerospace, civil and mechanical engineering infrastructures [25]. Damage can be defined as modifications in the material or changings on geometric properties of these systems. This whole process involves the observation of a structure over time and extract damage-sensitive features to analyze the current status of the system with the help of embedded FBG sensors [25]. These embedded FBG sensors can give information about the health of the structure.

● Etched fiber sensors (EFS) can be spliced inside the CRD loop. In EFS application, a small section of optical fiber is etched to ex-pose the core of the fiber to the environment. Etched fiber sensors can be used in fiber CRD loop for process monitoring of composite materials. When this etched region is surrounded by the resin flowing through the mold, the amount of attenuation in the received pulse may exhibit changes. These changes may give us aspect about curing process.

● In some sensing applications remote control may be required. Remote sensing may be realized by adding a mirror (to reflect the light signal back to the circulator) and another circulator inside the loop to let the pulse travel until the desired sensing point (see figure 4.1) [26]. In this kind of configuration, there will be a need for pulse with higher power to provide enough gain to get a reasonable decay time. This can be done by adding an erbium-doped fiber amplifier (EDFA) [26] to the loop as in figure 4.1.

Moreover, if multiple sensor heads can be inserted in a single sensor device, creating a multiple-parameter CRD sensor, the temperature and strain effects can be simultaneously measured.

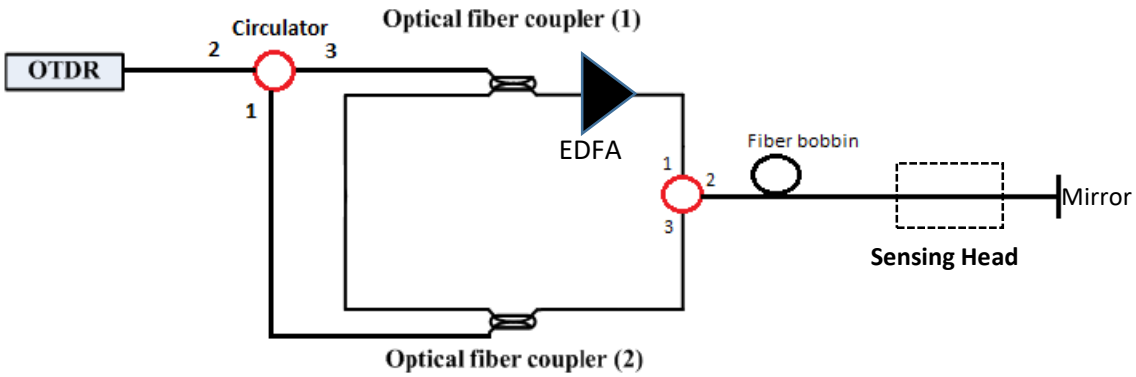

Figure 4.1. Fiber CRD loop for remote sensing applications

REFERENCES

[1] US Department of Energy, (February 2015), Quadrennial Technology review, CH8 "Advanced Composites Materials and their Manufacture Technology Assessment", from, http://energy.gov/sites/prod/files/2015/02/f19/QTR%20Ch8%20-%20Composite%20Materials%20and%20Manufacture%20Feb-13-2015.pdf

[2] Özdemir N. G. (2011) "An experimental study on the process monitoring of resin transfer molded composite structures using fiber optic sensors", Master Thesis, Sabanci University.

[3] Yüksel K. (2011) "Development of an optical frequency domain reflectometer and applications to the interrogation of fiber Bragg gratings'', Phd Thesis, Faculté Polytechnique de Mons.

[4] Li X., Yang C., Yang S. "Fiber-Optical Sensors: Basics and Applications in Multiphase Reactors", Optical Fiber Sensors, Vol. 12(9), 12519-1254, 2012.

[5] Caucheteur C. (2007) "Realization of mechanical and chemical sensors based on the fiber Bragg gratings technology,'', Phd Thesis, Faculté Polytechnique de Mons.

[6] Kashyap R., "Fiber Bragg Gratings,'' 1990.

[7] Erdoğan T., "Fiber grating spectra,'' Journal of Lightwave Technology, vol. 15, num. 8, pp. 1277–1294, 1997.

[8] Boz T. (2012) "Structural Health Monitoring of Composite Materials with FBG Sensors: Damage Detection and Remaining Useful Life Prediction", Master Thesis, Sabanci University.

[9] Yuan J., Zhao C., "A Fresnel reflection-based optical fiber sensor system for remote refractive index measurement using an OTDR ", Photonic Sensors, Volume 4, Issue 1, pp 48–52, 2014.

[10] Güneş M. D. (2013) "Development of process techniques for composite based leaf spring systems", Master Thesis, İzmir Instıtute of Technology.

[11] Farrel G., Ramakrishnan M., Semenova Y., “Optical Fiber Sensors for Smart Composite Materials and Structures”. In: Optical Fiber Sensors: Advanced Techniques and Application, 2015.

[12] David K. HSU. “Nondestructive inspection of composite structures: methods and practice”. In: 17th World Conference on Nondestructive Testing, 2008.

[13] Buggy S. J. (2008) “Composite material process monitoring using optical fibre grating sensors”, Phd Thesis, Cranfield University.

[14] Djordjevic B., “NONDESTRUCTIVE TEST TECHNOLOGY FOR THE COMPOSITES”. In: The 10th International Conference of the Slovenian Society for Non-Destructive Testing. Ed. by Materials and Inc. Sensors Technologies, 2009.

[15] Berden G., Peeters R., and Meijer G., “Cavity ring-down spectroscopy: Experimental schemes and applications,” Int. Rev. Phys. Chem., vol. 19, pp. 565-607, 2000.

[16] Silva S., Passos D. J., Marques M. B., Frazao O. “Fiber Cavity Ring-down for Strain Sensing Using an OTDR” Photonics Conference, 2014 Third Mediterranean IEEE.

[17] Passos D., Silva S.,Ferna J. R.A., J., Marques M. B., Frazao O. “Fiber Cavity Ring Down Using an Optical Time-Domain Reflectometer”, PHOTONIC SENSORS, Vol. 4, No. 4, 2014.

[18] Wang C., “Fiber ringdown temperature sensor,” Opt. Eng. Lett., vol. 44, no. 3, 030503, 2005.

[19] W. P. Tarsa D. M. Brzozowski, P. Rabinowitz, and K. K. Lehmann, “Cavity ring-down strain gauge,” Opt. Lett., vol. 29, no. 12, pp. 1339- 1341, 2004.

[20] Wang C. and Scherrer S. T., “Fiber ring-down pressure sensors,” Opt. Lett., vol. 29, no. 4, pp. 352-354, 2004.

[21] Wuilpart M., Thévenaz L., “Advanced Fiber Optics”, “Chapter 8: Rayleigh scattering in optical fibers and applications to distributed measurements”, CRC Press, ISBN 978-1-4398-3517-3, 205, 2011.

[22] Optical Time-Domain Reflectometer (OTDR) from

http://www.exfo.com/glossary/optical-time-domain-reflectometer-otdr

[23] Optical Time Domain Reflectometer (OTDR), The FOA Guide To Fiber Optics from

http://www.thefoa.org/tech/ref/testing/OTDR/OTDR.html

[24] Cengiz, B. (2013) "Fiber Loop Ring Down Spectroscopy For Trace Chemical Detection", Master Thesis, Middle East Technical University.

[25] Sorensen L. (2006) "The Response of Embedded FBG Sensors To Non-uniform Strains In CFRP Composites During Processing And Delamination", Master thesis, ÉCOLE POLYTECHNIQUE FÉDÉRALE DE LAUSANNE.

[26] Passos D., Silva S., R.A., J., Marques M. B., Frazao O. "A new cavity ring-down topology for remote sensing", Photonics Conference, 2014 Third Mediterranean IEEE.